A Multi-City Analysis of the Natural and Human Drivers of the Urban Heat Island

A THESIS
SUBMITTED TO THE FACULTY OF THE GRADUATE SCHOOL
OF THE UNIVERSITY OF MINNESOTA
BY

William Frederick Hertel

IN PARTIAL FULFILLMENT OF THE REQUIREMENTS
FOR THE DEGREE OF
MASTER OF SCIENCE

Advisors: Peter Snyder & Tracy Twine

August 2014

Acknowledgments

I'd also like to thank my advisors, Dr. Peter Snyder and Dr. Tracy Twine for their guidance throughout this process. Working with them was enjoyable and their help and mentoring were critical in reaching this point. Thank you to Keith Harding, Phillip Mykleby, and Brian Smoliak for occasionally providing a sounding board for ideas during my studies and research. To them and the rest of the group, Hong Xu, Stefan Liess, Tom Hultquist and Thiago dos Santos, thank you for providing a relaxed and productive atmosphere in which I could work and thrive.

I would like to thank my committee for helping to shape this thesis into its final form. I appreciate the assistance greatly. Thank you Dr. Snyder, Dr. Twine and Dr. Lawrence Baker.

I would also like to thank my parents, Bruce and Lynn, as well as the rest of my family and friends. Without all of your support and encouragement throughout this entire process I would not be here today.

Abstract

The world's population is increasingly moving to cities, with a present day urban population of over 3.6 billion that is expected to nearly double by 2050. One of the key features of the urban environment is an increase in temperature relative to the surrounding rural areas, called the urban heat island, which can have negative impacts on the health and wellbeing of urban dwellers. This study uses a novel approach of analyzing a large number of cities from around the world to investigate the similarities and differences in urban environments among cities to explore the behavior and drivers of the urban heat island. This methodology reveals two new conditions that increase the magnitude of the heat island - low dewpoint temperature and high air temperature. Many of the cities show increases in the magnitude of the heat island during hot or dry periods of 1.0 ˚C or more during the daytime and 2.0 ˚C at night relative to cool or humid periods. The heat wave results are of particular note due to the added stress on urban residents during periods when the population is already at risk. For cities in temperate climate regimes, differences among cities in vegetative cover or impervious surface area leads to increases in urban temperatures of up to 1.0 ˚C during the summer, while cities with high pollution can see reductions in the heat island by 1.5 ˚C. Cities in tropical or Mediterranean climates have the strongest heat islands during the dry season indicating that urban infrastructure is the key driver in these cities. These results indicate that mitigation of the urban heat island is possible by altering the urban landscape through changes in the urban vegetation and the structure of the built environment.

Table of Contents

Acknowledgments ..... **i**

Abstract ..... **ii**

Table of Contents ..... **iii**

List of Tables ..... **vi**

List of Figures ..... **vii**

Introduction **1**

1.1 Relevance of the Urban Heat Island **2**

1.2 Observed features of UHI **3**

1.3 Energetics of the UHI **5**

1.3.1 The Urban Energy Balance 5

1.3.2 Urban Geometry 6

1.3.3 Winds and Turbulence 7

1.3.4 Urban Surface Materials 8

1.3.5 Air Pollution 9

1.3.6 Anthropogenic Energy Use 11

1.3.7 Evapotranspiration 12

1.4 Difficulties in Understanding Heat Island Behavior **14**

1.4.1 Problems in Measuring the UHI 14

1.4.2 Limitations of Current Studies 15

1.4.3 Study Goals 16

Methods **18**

2.1 Data **19**

2.1.1 Data Acquisition 19

2.1.2 Station Classification 20

2.1.3 City Classification 21

2.2 Data Processing 23

2.2.1 UHI Metric Generation 23

2.2.2 Station Validation 23

2.2.3 Quantifying Meteorological Influences 24

2.2.4 UHI Comparison Among Cities 26

Results 30

3.1 Global Summary of UHI Behavior 31

3.1.1 Overview 31

3.1.2 Example heat islands 31

3.1.2.1 Tokyo, Japan 32

3.1.2.2 Phoenix, AZ 32

3.1.2.3 Paris, France 32

3.1.2.4 Recife, Brazil 33

3.2 Controls on UHI development 33

3.2.1 Latitudinal Controls 33

3.2.2 Meteorological Controls 35

3.2.2.1 Wind Speed 35

3.2.2.2 Sky Cover 35

3.2.2.3 Dew Point Temperature 36

3.2.2.4 Temperature 36

3.2.2.5 Precipitation 38

3.2.3 Environmental Factors 38

3.2.3.1 Population 38

3.2.3.2 Vegetation 39

3.2.3.3 Impervious Surfaces 39

3.2.3.4 Air Pollution 40

3.2.3.5 Combination of Environmental Factors 40

Discussion 42

Conclusions 51

5.1 Summary 52

5.2 Future Work 54

Tables 57

Figures 64

Bibliography 82

Appendix 88

A1. List of meteorological station IDs used from the Integrated Surface Hourly data set. 90

List of Tables

Table 1. Categories for assessing the UHI under contrasting meteorological conditions.57

Table 2. The average UHI (˚C) for each city on annual, winter (DJF in the Northern Hemisphere, JJA south), summer (JJA north, DJF south), daytime (1100 to 1600 local time), nighttime (2300-0400), summer night and winter night time periods. Maximum UHI for medium or high data quality cities for each column in bold. Low quality extremes greater than the higher quality maximum in italics. 60

Table 3. The number of cities with a significant difference ($p < 0.01$) in the mean UHI for the two meteorological conditions. Positive and negative UHI differentials are defined by the convention listed for each category. For temperature and dewpoint depression, the periods are limited to only those time periods where the sky cover was clear or scattered and the winds were less than 5 m/s. 61

Table 4. Correlation of UHI with environmental factors between cities. Correlations are calculated using medium and high quality cities for summer/winter nighttime UHI with clear/scattered skies and low winds. Data in presented for all extratropical cities and separately for temperate extratropical cities. * significant at $p > 0.1$ ** significant at $p > 0.05$..... 62

Table 5. Summer multiple variable regressions of environmental factors to UHI in temperate cities. The R^2 and the range of fitted values from the regression show the amount of influence the different variable combinations have on the UHI..... 63

List of Figures

Figure 1. Cities in study 64

Figure 2. Station classification examples 65

Figure 3. Heat island temporal maps for selected cities 66

Figure 4. Summer UHI and insolation by city 67

Figure 5. Heating rate and UHI development 68

Figure 6. Difference between each city's winter nighttime UHI and summer nighttime UHIs plotted by latitude. 69

Figure 7. Minneapolis-Saint Paul, MN nighttime UHI and wind speed 70

Figure 8. Chicago, IL UHI and sky cover 71

Figure 9. Atlanta, GA UHI and dewpoint temperature 72

Figure 10. New York City, NY summer daytime UHI and temperature 73

Figure 11. New York City, NY UHI and temperature 74

Figure 12. Winter night UHI difference between warm events and cold events by mean winter temperature 75

Figure 13. Precipitation and UHI correlation by latitude and biome 76

Figure 14. Mexico City, Mexico individual month UHI and precipitation 77

Figure 15. Average winter nighttime UHI of extratropical cities and population, grouped by biome with linear regression trend for all cities. 78

Figure 16. Average winter nighttime UHI of extratropical cities and population density, grouped by biome with linear regression trend for all cities. 78

Figure 17. Summer monthly rural NDVI and nocturnal UHI for (a) all biomes and (b) temperate cities with linear regression trend. 79

Figure 18. Summer monthly rural – urban NDVI difference and nocturnal UHI for all cities with linear regression trend. 79

Figure 19. Impervious surface fraction and summer nocturnal UHI for all cities with linear regression trend. 80

Figure 20. Average winter nighttime UHI of extratropical cities and impervious surface fraction, grouped by biome with linear regression trend for all cities. 80

Figure 21. PM10 air pollution and summer nocturnal UHI for all cities with linear regression trend. 81

Chapter 1

Introduction

1.1 Relevance of the Urban Heat Island

The world's population has changed significantly since the beginning of the 20th century. In 1900 only 10% of the world's population resided in cites while now more than 50% of the world's inhabitants are considered urban dwellers (Grimm et al. 2008). This growth in urban population is projected to continue into the future, with the urban residential population of 3.6 billion in 2011 increasing to 6.3 billion in 2050, driven largely by continued population growth and urbanization in the less developed regions of Asia and Africa (UN 2011). Urban development leads to major alterations to the local environment including the air above it. The urban built environment contributes to local increases in air temperature in urban regions relative to the surrounding rural regions, known as the urban heat island (UHI). This phenomenon was first described by Luke Howard in the early 1800s (Howard 1833) and first named the urban heat island by Manley (1958). This feature has been observed for air temperature in both the canopy and boundary layers as well as the surface skin temperature.

The urban heat island increases the temperature within a city, often leading to negative consequences for the local population. Meteorological events like heat waves lead to increased mortality (Curriero et al. 2002), such as those that affected France in 2003, resulting in 15000 excess deaths (Fouillet et al. 2006), and Chicago in 1995, resulting in 739 additional deaths (Whitman et al. 1997). In the case of the 2003 European heat wave the increased nighttime minimum temperatures in various parts of Paris due to the heat island have been shown to correlate with changes in the mortality rate for each sector (Laaidi et al. 2012). Heat waves and the urban heat island can have

additive effects as heat rejection from buildings from increased air conditioner use during major events can lead to a temperature increase of 0.5 ˚C or more at street level (Salamanca et al. 2014; Tremeac et al. 2012). High urban temperatures can also drive increases in air pollution, as ozone production has been shown to scale with temperature (Stone 2005). Additional heat in urban areas can also drive increased energy demand (Taha et al. 1999) although this effect can be dependent on a city's climate and the energy and heat efficiency of its buildings (Hirano; Fujita 2012). The heat island also varies within a city and may have unequal effects along socioeconomic lines as a study in Phoenix, USA showed that the strength of the heat island increased as median home value decreased (Jenerette et al. 2007). As urban population growth continues and cities get larger, the UHI and its impacts on local populations will continue to grow in significance.

1.2 Observed features of UHI

Studies of a variety of urban climates have been used to identify some common features of heat islands. The urban heat island manifests itself with increased daily average, minimum and maximum air temperatures (Karl et al. 1988). One of the primary observed features of the urban heat island is that it has a stronger nocturnal, rather than daytime, magnitude (Oke 1982), which also implies a decreased diurnal temperature range within cities (Karl et al. 1988). This nocturnal effect is noted by a rapid increase in the UHI magnitude around sunset, and then a decrease around sunrise (Holmer et al. 2007; Oke 1982). The transition between nocturnal and daytime phases of the UHI is driven by heating and cooling rates for rural areas that are greater than for the urban area,

particularly in the periods after sunrise and sunset, respectively (Holmer et al. 2007; Johnson 1985; Oke 1982). Another primary feature of urban heat islands is that more populous cities provide greater modifications of the environment leading to larger heat island magnitudes. Karl et al. (1988) generated population-based regressions for UHI magnitude in cities in the United States and showed that the heat island grows with the population to the power of 0.45 from small towns to large cities. Other regions of the world can show different rates of change in the UHI magnitude with respect to the population, although the trend is always positive (Oke 1982; Park 1986). The strength of the heat island within a city can also vary as the urban form varies, with more densely developed or less vegetated regions experiencing greater warming. A study in New York City found that the urban temperature varies by as much as 2 ˚C between sites within the city (Gaffin et al. 2008).

Meteorological factors such as the general climate of a city and synoptic weather patterns can also influence the development of the heat island, or in some cases overwhelm or eliminate it. (Landsberg 1981). Reviews by Souch and Grimmond (2006) and Arnfield (2003) provide multiple examples of individual city urban heat islands that demonstrate decreasing temperature differentials with increasing wind speed, a result of the urban and rural air mixing and enhanced turbulent transport of the heated urban air away from the surface. Studies have also shown that increased cloud cover decreases the magnitude of the UHI (Arnfield 2003; Souch; Grimmond 2006). Morris (2001) suggests the relationship is due to urban features having greater influence during clear sky periods than when clouds limit radiative cooling. High-pressure conditions have been shown to

occur during stronger heat island events, largely because those conditions contribute to lower winds and reduced cloud cover that lead to stronger heat island development (Morris; Simmonds 2000). However, the seasonal variability of heat island development is not clear, with numerous studies providing conflicting views. Souch and Grimmond (2006) comment that the UHI "is least developed in summer," while Arnfield (2003) notes that UHI is best developed in the warm half of the year, with both reviews referencing multiple studies to support their assessments.

The nature of the biome in which a city resides defines the rural background, thus influencing heat island development. Forested regions with high evapotranspiration (ET) rates, especially in the summer effectively cool the rural region, resulting in greater changes to the surface energy balance and a stronger heat island (Imhoff et al. 2010). In contrast arid and semi arid regions can show an "oasis effect" in which the daytime temperatures are cooler in the urban region than in the surrounding desert due to an increase in ET from parks and lawns in the urban and suburban region (Brazel et al. 2000).

1.3 Energetics of the UHI

1.3.1 The Urban Energy Balance

The primary factors driving the development of urban heat islands are the changes in the surface energy balance resulting from changes in surface geometry, materials and energy use brought on by urbanization. The energy balance (in W m^{-2}) for an urban area can be described as:

$$Q^* + Q_F = Q_H + Q_E + \Delta Q_S + \Delta Q_A$$

Where Q^* is net radiation, Q_F is anthropogenic heat release, Q_H is sensible heat, Q_E is latent heat, ΔQ_S is the change in surface heat storage and ΔQ_A is the net heat energy advected out of the area. Anthropogenic modification to the landscape in urban regions alters the terms of the surface energy balance, resulting in an increase in the amount of energy expressed as sensible heat and changing the air temperature.

1.3.2 Urban Geometry

The placement of buildings and streets in the urban landscape introduces a faceted canyon geometry that alters the radiation balance of the surface. This new geometry reduces the fraction of longwave radiation emitted by the urban skin that can escape the canopy layer due to interception by other facets of the canyon (Oke 1982). This weakens the normal radiative cooling process of the urban surface leading to an increase in trapped energy within the canopy layer. This has led to research into quantifying the trapping potential of the urban form represented by the sky view factor (SVF) which is the "fraction of the overlying hemisphere occupied by the sky" (Oke 1981). Oke showed that the decrease in outgoing longwave radiation due to a lower sky view factor plays a role in the development of the nocturnal heat island. There have been efforts to derive observational relationships between the magnitude of the heat island and the sky view factor for individual locations within cities, but results vary between cities and even from district to district within them as the variability of the ratio of building height and canyon width between a tall building district and low density housing results in very different sky view factors (Unger 2004). Within a city, regions with a more restricted sky view factor

show the biggest decrease in cooling rates during the period around sunset (Holmer et al. 2007).

In addition to limiting longwave energy release, the canyon geometry also influences the heat island by effectively decreasing the urban albedo. Surface reflection of shortwave radiation in the urban canopy is more likely to intersect with another surface than in rural areas, providing additional opportunities for radiation to be absorbed. Tower and aerial measurements of urban and suburban regions have shown lower albedos than the rural areas surrounding cities (Christen; Vogt 2004; Oke 1988). This decrease in albedo results in increased shortwave absorption for an urban area, increasing the energy available at the surface. In high latitude cities, snowfall can further increase the urban/rural albedo differential, with snow removal, soiling and vertical walls all reducing the urban albedo significantly relative to rural settings (Oke 1988). The variation in the urban form within a city can lead to changes in albedo as the structure of the city changes. Modeled results of various regions indicate that the albedo of the urban core can be much lower than the albedo in residential areas of a city (Sailor; Fan 2002). This can result in regional variability in the UHI as denser European cities can absorb more shortwave energy than the more spatially expansive American cities (Christen; Vogt 2004).

1.3.3 Winds and Turbulence

Winds moving through an urban region can transport energy between urban and rural air masses, but this impact on the urban scale temperature within the canopy is limited (Oke 1988). Cities are areas of increased turbulent energy transfer due to the high

surface roughness of the urban region, although this effect is mitigated within the canopy because of decreased wind speeds (Oke 1987). Increased roughness in urban areas from the urban development (e.g., buildings, lawns and interspersed trees) results in low wind speeds within the canopy and urban canyons, limiting the ability of heat near the surface to mix into the boundary layer above it (Oke 1982). As wind speeds and thus turbulence increase, the increased advection and mixing of the urban air mass reduces the UHI. Investigation into the UHI of Seoul, South Korea found that the UHI ceased to exist above a critical wind speed of 11.1 m s^{-1} with smaller cities in the region having lower critical wind speeds (Park 1986). In studying this impact, properly modeling the roughness heights for urban areas has been difficult because differing approaches result in dissimilar roughness parameters, with little evidence of a best method. Because of this difficulty, attempts to model and understand the impacts of turbulence remain a challenge (Arnfield 2003).

1.3.4 Urban Surface Materials

The exposed surfaces in urban areas have a greater thermal admittance than in rural areas changing the surface storage term of the energy balance. The urban surfaces absorb more energy over the course of the day than the rural environment, and release the additional energy back into the canopy layer at night (Kanda 2007). Directly measuring this energy flux is difficult as aggregating heat flux observations in an urban region is not feasible (Arnfield 2003) resulting in some uncertainty in empirical understanding of the contribution of heat storage to the heat island. The average thermal admittance of urban and rural materials is generally similar (Oke 1981, 1988), however, studies have

determined that the thermal admittance of the urban landscape does play a role in the urban energy balance. Grimmond and Oke (1999) investigated the storage in urban landscapes through the residual of $Q^* - (Q_H + Q_E)$ and found that the storage was significant in the energy balance and inversely correlated with vegetation. The study also showed that cities that had net daily heat storage in summertime and heat loss in wintertime as the subsurface levels warm in the summer and cool throughout the winter. Defining the storage term as the remnant after removing sensible and latent heat is an issue as it not only compounds the errors in both those measurements, but also neglects the influence of anthropogenic heat and advection, both of which can be significant in an urban environment (Kanda 2007). Experimental scale model (Pearlmutter et al. 2005) and numerical (Arnfield; Grimmond 1998) studies have shown that there is significant interplay between heat storage and the canyon geometry, with deeper canyons resulting in greater heat storage. Thermal admittance can also be relevant in the rural areas around a city, as regions with a wet/dry seasonal cycle show variability in the heat island as a result of increases in the heat capacity of wet soils compared to dry soils. Mexico City shows a weaker heat island in the wet season which has been at least partially attributed to changes in rural thermal admittance due to greater soil moisture during the wet season (Jauregui 1997).

1.3.5 Air Pollution

Measurements have shown that surface shortwave radiation received in urban areas can be reduced by 10 to 30% relative to rural areas (Oke 1988). This reduction in incoming surface radiation means that the urban landscape has less total energy driving

the surface energy balance, limiting the development of the UHI. This effect varies between cities as total pollution and particulate size change. Different particulate sizes influence radiation differently, with large pollution particles increasing the absorption and reflection of shortwave light leading to greater attenuation of sunlight, while smaller particulates (such as in photochemical smog) primarily contribute to forward scattering effects that alter the diffuse/direct beam ratio at the surface. This leads to greater attenuation of sunlight in cities with higher large particulate air pollution (Oke 1988). This effect can influence how heat islands develop in various regions of the world, as particulate pollution levels tend to vary by country, with cities in North America and northern Europe having lower average PM10 levels than Asian or Central and South American cities (WHO 2011). Studies have shown a strong reduction in shortwave radiation received at the surface in heavily polluted cities. Jaurengi and Luyando (1999) recorded average attenuation over 21% for Mexico City during the dry season, with peak values as high as 35% with calm winds. Hong Kong has shown a reduction in solar radiation of 33% since 1950 after controlling for cloud cover changes (Stanhill; Kalma 1995). The increased pollution in urban areas also increases the emissivity of the boundary layer, leading to greater longwave emission back to the surface (Oke 1982). However, the importance of pollution's influence on longwave emissions to the surface is difficult to assess because increased boundary layer temperatures in urban areas will also increase the longwave radiation received at the surface, and demonstrating the influence of air pollution on longwave radiation has proved difficult. Estournel et al. (1983) found an increase in downward longwave radiation, but attributed it to an increase in boundary

layer temperatures within the urban heat island, rather than changes in atmospheric emissivity due to the presence of pollutants in the urban atmosphere.

1.3.6 Anthropogenic Energy Use

Anthropogenic heat release from human activity adds additional energy to the urban core that is not present in outlying rural areas. The source of this energy is primarily building energy consumption and transportation, with human metabolic energy representing less that 5% of the energy load for a city (Sailor; Lu 2004). People moving into the city core during working hours can increase the energy usage as city populations within the U.S. can increase by 50 to 100% during working daytimes and commercial districts can see population densities 30x the city average (Sailor; Lu 2004). On the district scale this added energy can be extremely significant as Tokyo has demonstrated blocks with anthropogenic energy release that peak as high as 1590 W m^{-2} in winter early morning hours (Ichinose 1999). These high values of energy released per area in the tall building districts are somewhat mitigated by a large spread in the vertical distribution of the energy discharged (Sailor 2011). On larger city scales, the influence of anthropogenic heat is more diffuse but still significant. Sailor and Hart (2006) estimate that the citywide winter anthropogenic heat flux for New York City ranges from 85 to 96 W m^{-2} during the daytime, with other less densely populated cities having lower values. This can be an important factor, particularly in winter, for the differential heating between urban and rural areas. In the case of New York City the limited solar input during winter means that the anthropogenic energy additions are an appreciable fraction of the total energy balance in the urban area. Ichinose (1999) also demonstrates that for a highly built up region of

Tokyo in the winter, the total daily energy supplied by shortwave radiation and anthropogenic sources can be similar. Ichinose also suggested that in heavily built up areas anthropogenic heat could increase the Tokyo heat island by over 1.0 ˚C. The anthropogenic load in a city varies on annual time scales, as heating and cooling needs vary by season, and the structure of this load can vary strongly by climate as a high latitude city has much higher energy usage for winter heating than summer cooling, while a lower latitude city has reversed energy use. The anthropogenic heating loads also vary on shorter time scales, with diurnal and weekly cycles as commercial districts have high energy loads during working week daytimes, and residential neighborhoods have the reverse the pattern (Sailor 2011). Because much of the energy use in cities is confined within building, the transfer of energy loads to the external environment can be delayed by factors such as insulation, altering the timing of sensible heat emissions to the environment (Ichinose et al. 1999; Sailor 2011). One aspect of anthropogenic heat release that may limit temperature increases is that a portion of the transportation and building energy is released as latent heat from combustion and evaporative cooling respectively (Sailor 2011) although this may alter apparent heat indices.

1.3.7 Evapotranspiration

Evapotranspiration (ET) in the urban system is altered due to less expansive vegetation, increased impervious surface area, and greater runoff in the urban region relative to the rural background. Studies have shown a relationship between the surface vegetative area and the evapotranspiration in an urban region (Christen; Vogt 2004). This relationship is not always the simple trend that less vegetation yields lower ET rates as

irrigation effects in urban regions can offset the reduction in vegetated area. This can be especially true during dry events when rural vegetation is highly water limited while much of the vegetation in urban areas may receive irrigation (Arnfield 2003). Seasonal ET rates in urban areas may also be altered by the heat island as studies have suggested that the UHI extends the growing season in colder regions, which can extend the period of active vegetative ET earlier in spring and latter into the fall (Imhoff et al. 2004; Peters et al. 2011). ET measured over irrigated lawns has been shown to be capable of exceeding the theoretical potential ET due to advection of hot dry air from nearby impervious surfaces driving a stronger latent energy flux (Oke 1982). Studies have also shown that sparse urban vegetation can have greater ET rates per unit area than denser vegetation, meaning that extrapolating based on areal average vegetation may underestimate urban ET (Moriwaki; Kanda 2004). These effects indicate that the relationship between the latent energy flux and the fraction of urban vegetation coverage is not as direct as might be assumed, and models that strongly relate vegetative fraction to UHI may not be ideal (Kanda 2007). The impact of urban vegetation levels and ET influence the UHI are also dependent on the rural surroundings. Arid and semi arid regions have less vegetation in rural areas than regions with greater rainfall, leading to an urban landscape with less deviation from the rural landscape than in wetter regions, which can lead to a weaker UHI (Imhoff et al. 2010). Temperate cities located in more heavily vegetated biomes have shown much stronger UHIs in summer than in winter, partially described by the difference in the evaporative cooling rates (Imhoff et al. 2010).

Changes in vegetation amounts within different districts of a city can also result in variations in the local UHI (Jenerette et al. 2011; Jenerette et al. 2007).

1.4 Difficulties in Understanding Heat Island Behavior

1.4.1 Problems in Measuring the UHI

One issue that has plagued urban heat island studies is defining and measuring the urban heat island for a city. While the concept of the urban-rural temperature difference is straightforward the establishment of urban and rural sites to define those points is more problematic. Sociologists have suggested that the definitions of urban and rural are insufficient, particularly within Asia and the developing world (Montgomery 2008). Changes in urbanization patterns in these regions have lead to a coexistence of urban and rural features, making the countryside around an urban core to be less "rural" that the traditional definition (Lin 1994; Stewart; Oke 2012). These shifts can be compounded by large cities urbanizing the entirety of the geographical region in which they reside. Tokyo has expanded to the point that "it is no exaggeration to say that the whole area of the Kanto Plain… is more or less urbanized"(Yamashita 1990). In addition to the difficulty in selecting rural sites, the urban site selection is also fraught with difficulty. The land use of cities tends to be heterogeneous, leading to differing surface characteristics that present varied strengths of localized heat island development. As a result the local heat island can vary appreciably within a city as sites in New York City show variation of up to 2 ˚C in UHI magnitude between stations that are only 5 km apart (Gaffin et al. 2008). Stewart and Oke (2012) proposed ten different local climate zone categories of urban land use to address the heterogeneity of cities. They provide approximate values of

surface thermal admittance, albedo and anthropogenic heat for each category to show how each zone can alter the urban energy balance and drive heat island development. Urban and rural site selection can also be complicated by factors outside of the urban rural landscape difference. Changes in proximity to water, such as a sea breeze moderated urban site with a more inland rural site that is not affected by the sea breeze would result in influences on the measured temperature difference that are unrelated to the UHI (Yamashita 1990). Elevation and latitude differences between nearby urban and rural site may also introduce differences in the temperature of the sites that are unrelated to the urban form (Peterson 2003) although local microclimate differences may overwhelm these factors (Gallo 2005).

Another aspect that makes assessment of the heat island more difficult is the temporal variability of measurements. Many studies of heat islands use maximum and minimum temperatures which are not necessarily synchronized in time between urban and rural sites, leading to an inadequate representation of actual magnitude of the heat island (Stewart 2011). Frontal passages can also generate inaccurate measurements of the UHI, as measurements made during a cold front passage can generate an urban-rural divergence of temperature greater than the maximum UHI under ideal conditions that are unrelated to urban form because urban and rural stations are on opposing sides of the front (Szymanowski 2005).

1.4.2 Limitations of Current Studies

Most studies of urban heat islands focus on single cities, however, there are some that focus on a number of cities, although these also are somewhat limited. Many of these

studies limit the study area to a single county, such as Karl (1988), Stone (2007) and Mishra and Lettenmaier (2011) investigating cities within the United States. Some of these studies are also focused on determining long term trends in urban temperatures, which can introduce additional complexity as a multitude of variables are needed for analysis, including changes in population, city structure, as well as long term climate trends which are independent of the urban form. This results in an incomplete picture of how heat islands develop on a global scale, and makes it difficult to assess how changes in features like city structure or latitude might affect heat island development.

1.4.3 Study Goals

The goal of this study is to investigate the nature of the urban heat island in 64 large cities around the world to understand how the traits of urban environments influence heat island development. Hourly measurements of temperature at multiple stations in and around cities are used to better understand how the UHI varies for each city on diurnal and annual time scales. This study also assesses the meteorological, environmental and anthropogenic factors that change the energy balance for urban regions and drive heat island development. The impact of meteorological conditions including sky cover, wind speed, precipitation and dewpoint temperature are evaluated to assess the impact of those weather conditions on the UHI of each city. The influences of weather conditions are assessed through both changes in the average UHI under categorized conditions for each variable and through the correlation between UHI and each weather variable at any point in time. This study furthers our knowledge of the development of heat islands by investigating the influence of local environmental and

anthropogenic factors on the UHI of selected cities. The use of many cities provides the ability to correlate the changes in the UHI with the changes in the physical attributes of the cities. This provides the ability to determine which physical elements most strongly drive heat island development and provide the greatest opportunity for developing mitigation strategies that work. The impact of differing rural backgrounds is also addressed by categorizing the cities by rural biome, and by comparing the UHI with the local rural vegetation levels.

Chapter 2

Methods

2.1 Data

2.1.1 Data Acquisition

The list of urban agglomerations—one definition to delineate the population and borders of an urban region—from the United Nations World Urbanization Prospects (UN 2011) was used to create a list of the largest cities to use as candidate urban regions for analysis. The Integrated Surface Global Hourly (ISH) dataset from the National Climatic Data Center (NCDC) was used to obtain hourly data for urban and rural sites in the vicinity of these cities (National Climatic Data Center/NESDIS/NOAA/U.S. Department of Commerce 2005). The ISH data set contains meteorological data on one or three hour intervals (depending on country) and includes temperature, dewpoint temperature, wind direction, wind speed, pressure and sky cover.

The cities in the candidate list were compared to the list of stations in the ISH dataset to determine which regions that had stations both within the urbanized region and in rural areas within a radius of 150 km of the urban center. After data retrieval and processing, 64 cities had sufficient quality and quantity of data to be used in the analysis. (Fig. 1) For cities that met the criteria the hourly data were obtained for all stations in and around the urban centers for the time period of 2000 through 2012, or for as long as the data was available within that timeframe. The duration of the data period was limited to this 13-year span to limit trends from changes in population, urban infrastructure or climate, while still providing sufficient data points to provide statistical significance and limit the impact of short-term weather anomalies. To correct for variations in station temperature due to elevation differences between sites, station temperatures were

corrected using a lapse rate of -5.3 ˚C/km (Berry et al. 1945). The elevation correction is fairly small for most cities as the difference between the average rural station elevation and the average urban station elevation was less than 50 m for two thirds of the cities, but eight of the cities had elevation differences in excess of 94 m.

2.1.2 Station Classification

Individual sites were initially defined as rural, urban, or intermediate (suburban) based on parameters including distance from the urban center, MODIS (MODerate-resolution Imaging Spectroradiometer) Normalized Differential Vegetation Index (NDVI) data (Huete et al. 2002), impervious fraction utilizing the National Geophysical Data Center (NGDC) Impervious Surface 2010 dataset (Elvidge et al. 2007), and a global map of urban extent (Schneider et al. 2009, 2010). Stations within the main urban areas from the global urban extent dataset were classified as urban, while sites not near large urban areas were classified as rural. For stations in outlying areas that were in or near smaller urban cells in the urban extent dataset, the impervious surface and NDVI datasets were used to assist in the assessment of the site. For sites where the local vegetation levels (determined by NDVI) were largely similar to the rural regions and the impervious surface fraction remained low, the sites were placed in the rural classification, while sites that showed greater deviation in impervious surface area or NDVI from the rural values were assigned to the suburban class. Special care was taken in the station selection process for cities near large bodies of water so as to minimize the variability between urban and rural stations imparted by sea breezes or other mitigating effects from proximity to water that are unrelated to urban development. To limit these influences,

urban and rural stations were chosen where the average station distance to water was not markedly different between the urban and rural groups.

2.1.3 City Classification

The cities were classified according to the biome, or background climate and vegetation. The map of terrestrial ecoregions, or biomes, from Olson et al. (2001) was used to define the biome that each city occupied. The cities were then grouped into Tropical, Arid, Mediterranean or Temperate climates categories. All cities located between 23˚N and 23˚S were qualified as Tropical to avoid issues with seasonality when compared to higher latitude cities. Cities that fell within the Desert and Xeric Shrublands biome were classified as Arid. The remaining cities primarily fell into various forest or grassland biomes and were placed into the Temperate category, which represents climates with sufficient moisture to allow extensive rural vegetation. While cities in Mediterranean biomes usually have sufficient vegetation to qualify for the Temperate category, the reversed seasonality of the precipitation led to separate categorization so intercity comparisons could be made without being influenced by the timing of the growing season.

The cities in the study were classified as having high, medium or low quality data due to variability in the available station data for each city that could limit how well the UHI data represented the true magnitude of the heat island of a city. This determination was made due to the large variability of the number of available urban and rural stations for each city and the representativeness of those stations. More developed countries tend to have denser temperature networks available, resulting in more quality sites that could

be used to generate a reliable UHI dataset. Cities that presented only a single option for urban and rural stations were classified as low quality, as they provided little opportunity to validate the quality or representativeness of station locations. Some cities were also classified as low quality if the most central urban station available was well away from the urban core, particularly if the impervious fraction was much lower than the core. Cities with only a few urban or rural stations available where the stations in either group did not behave consistently with each other were also qualified as having low quality due to the high variability of the data. Cities with multiple urban and rural stations that presented at least one quality station for each group were classified as medium quality. Cities with many stations available in urban and rural regions with multiple quality stations for use were classified as having high quality data. Figure 2 provides examples of this process with the high data quality urban regions of Tokyo and Minneapolis – Saint Paul showing large numbers of stations to choose from, which allows for the most representative stations to be used for urban and rural sites. In the case of Minsk, fewer stations were available, including only one urban station, but quality urban and rural stations were still available in proximity to the city, allowing a medium quality classification. Saint Petersburg had only three possible stations to use and the two rural stations are well over 100 km away from the city, leading to a low quality classification. The cities with low quality data were useful for determining patterns within the cities such as timing of maximum UHI and the impact of meteorological influences. For comparisons of UHI magnitude between cities, the low data quality cities were not used because of uncertainty in how well the data would represent the actual heat island values.

2.2 Data Processing

2.2.1 UHI Metric Generation

The hourly station data was processed by averaging the temperatures at each time within the urban and rural station groups to create average urban and rural timelines for each city. The averaging of multiple urban and rural sites for each city (when possible) limits the local siting effects that can cause variation in the measured urban (or rural) temperature and produces a value that can be more indicative of the average urban or rural temperature. The rural data series was then subtracted from the urban series to create a time series of the measured urban heat island for a city. This series was then processed to generate a matrix of the average UHI for each combination of month of the year and hour of the day. Average magnitudes for the UHI across the annual and diurnal cycles were also compiled. The annual cycle was grouped into the full year, monthly and the meteorological seasons (e.g., June-July-August) periods, and the diurnal cycle was grouped by the 24-hour day, daytime (1100-1600 local time) and nighttime (2300-0500) periods. The average UHI values were also generated for each combination of the annual and diurnal periods (e.g., summer nighttime, winter full day).

2.2.2 Station Validation

As a method of validating the station category assignments, the same method of generating the UHI metrics was used to compare the sites within each category. Each site within an urban or rural category for each city was defined as an “urban” site and the UHI metrics were created using the remaining sites are the “rural” background. This method allows the comparison of each site to be assessed against the others in the group

for differences indicative of a problematic site or improper categorization. Sites that deviated from the rest of the group were analyzed to determine the nature of the deviation, and in cases where the deviation pattern was either significantly cooler (for urban) or warmer (for rural) the site was relegated to the suburban pool. Sites that showed variability that strongly deviated from other nearby stations (for example, one site near Tokyo was more than 5˚C colder than other nearby rural sites during winter nights) were classified as problematic and not used in the analysis. Sites were also reclassified as suburban if a rural site showed temporal variations matching the pattern of the UHI for the city or if an urban site indicated the reversed pattern. Additionally, sites that were initially classified as suburban but had been borderline assignments to being urban or rural, were tested against the appropriate group to verify the initial assignment or to reclassify them into the urban or rural groups if the temperature signature indicated that the station was appropriate for those categories. These refinements created an improved selection of urban and rural sites for each city. Once the station selection was refined, UHI metrics for each city were regenerated.

2.2.3 Quantifying Meteorological Influences

Because local meteorology can influence the development of the heat island for cities, the data was also processed to analyze how difference meteorological factors influenced the heat island magnitude. A primary site was identified for each location (most frequently the main airport for the city) to use as the primary station for meteorological data (besides temperature). The meteorological conditions that were investigated include:

- Sky cover (clear, scattered, broken, overcast)

- Wind speed (above/below threshold speeds of 3 and 5 m s^{-1})
- Dewpoint temperature and dewpoint depression (temperature – dewpoint temperature)
- Air temperature

The creation of the urban and rural and UHI time series was performed again using the using the site to limit the time series to only those periods where the weather parameter of interest fell within the desired range. The average UHI metrics were then generated for all cities on this limited set. The difference between related conditions (i.e. low wind versus high wind) was then calculated to create difference matrices to assess how each condition influenced UHI structure. To determine the significance of changes in the UHI between the two sets a two-sample t-test was performed to determine if the difference between the two sets at each month/hour pair was different from 0 at the 95% significance level. As a method of determining the influence of land and sea breezes and wind direction on the UHI of coastal cities, the UHI metrics were collected for periods where the wind represented land and sea breezes separately and compared to assess any differences between the two conditions.

The impact of a specific meteorological condition was also examined by several methods. Criteria were defined for each meteorological variable to establish contrasting conditions as specified in Table 1. The average heat island under each meteorological condition was calculated and the difference between the two conditions was determined along with the significance of the difference, using a 99% significance test. This significance threshold was used to limit the number of false positives since there are 67

separate assessments for each meteorological variable. With this assessment, the cities were then classified as having a stronger heat island under one of the two conditions, or an inconclusive result. The response of the UHI to weather conditions was also assessed by calculating the correlation coefficient between the magnitude of the UHI and each of the meteorological variables in the time series. This was performed for wind speed, dewpoint temperature, temperature and sky cover. For the case of sky cover where the observed data is recorded in the ISH dataset as text between clear and overcast the values were converted to numeric values between 1 (CLR) and 4 (OVC) to perform the calculations.

To assess the influences of precipitation on the UHI, monthly precipitation data was downloaded from the NCDC over the 2000 to 2012 time period for each of the cities in the study. This data was then compared with the nighttime monthly UHI data using both all time periods and only during clear or scattered skies and low winds, to eliminate the variability in sky cover introduced by wet and dry months. The correlations between average monthly rainfall and monthly UHI magnitude were also generated for each city.

2.2.4 UHI Comparison Among Cities

The importance of local environmental features and urban landscape changes on the magnitude of the heat island was investigated by comparing the intensity of each city's UHI with the various local factors specific to each city. The value of each environmental factor for each city was determined and then the correlation between the nighttime UHI and the environmental factors was found across the set of medium and high quality data cities.

Environmental and urban features that were investigated include:

- Population - data based on UN list used to create the list of cities (2011)
- Population density – data for the central city region from the SEDAC Gridded population of the World v3 (Center for International Earth Science Information Network - CIESIN - Columbia University; Centro Internacional de Agricultura Tropical - CIAT 2005)
- Normalized Differential Vegetation Index (NDVI) as an indicator of vegetation greenness in and around a city with both urban and rural measurements. NDVI data was acquired from the MODIS MOD13A3 dataset. Satellite derived NDVI from both the Terra and Aqua satellites was retrieved for the months of June, July and August for Northern Hemisphere cities and December, January and February for Southern Hemisphere cities for the years 2000 though 2012 (Huete et al. 2002).
- Impervious Surface Fraction - Impervious surface data from NOAA NGDC (Earth Observation Group (EOG), National Geophysical Data Center (Elvidge et al. 2007))
- Air pollution - Annual average PM10 (particulate matter ≤ 10 μm) data from the World Health Organization (2011)
- Wind speed – average wind speed data at the primary station for each city using the ISH dataset.
- Latitude, length of day and total solar insolation - derived from latitude

Population, pollution, wind speed, latitude, length of day and solar insolation are variables that exist as citywide values for each city and did not require further processing. The population density, NDVI, and impervious surface data are raster based data sets that provided information about the variability of the urban form, and required processing to derive an areal average for each city, which was performed with ArcGIS. The city centers were initially defined by latitude/longitude coordinates in the UN list, with some cities requiring slight alteration to the defined center so that areal averages for the city would center on the most impervious/least vegetated areas of the city and to minimize the water fraction for cities near large bodies of water. A circular region with a 10 km radius was defined around each city center. Circular regions with a 2 km radius were also defined around each of the observation stations to permit assessment based on more localized urban site locations, which was not always in the densest, most impervious or least vegetated areas of a city. The raster data was averaged within each defined area using the ArcGIS Zonal Statistics tool to create single values for each city and station. For the NDVI data, which covers multiple time periods of data, the averaging was performed for each month and year time step and averaged across the Terra and Aqua satellites to create NDVI data points at each city and station. The data was also averaged across the time range to create a single NDVI value for the summer months at each location. Impervious surface fraction and population density only required the area average processing. For the smaller station site areas, all the urban sites and rural sites were averaged together to create composite urban and rural values representing the

observation station average for each city as well as the difference between the urban and rural values.

The seasonal nighttime heat island magnitudes during clear, low wind conditions across all of the cities were correlated with the factors listed above for each city. This process was also performed after grouping the cities by biome to assess how well each factor correlates to UHI for urban regions within similar rural conditions. For NDVI and impervious surface fraction, this process was performed using the localized station area data and with the larger urban core value to assess impact of vegetation on UHI on both a citywide and more localized scale. This was performed with each of the 10 km urban averages, the 2 km average around urban sites, the 2 km average around rural sites and the difference between the urban and rural site averages to assess the impact large urban scale vegetation, smaller more station dependent scales, the rural vegetation and the urban rural differential in vegetation.

Chapter 3

Results

3.1 Global Summary of UHI Behavior

3.1.1 Overview

The annual average heat island magnitude for all cities ranges from 2.14 ˚C for Phoenix, AZ, USA to a minimum of -0.39 ˚C for Sao Paulo, Brazil with an average of 1.00 ˚C across all cities (Table 2). For medium and high data quality cities, Manila has the lowest annual UHI at 0.48 ˚C, while the average for all cities is 1.23 ˚C. The diurnal variation in the UHI is pronounced with an average nighttime heat island for all cities of 1.62 ˚C greatly exceeding the daytime average of 0.23 ˚C. For medium and high data quality cities the averages are 1.89 ˚C at night and 0.40 ˚C during the day. All of the cities that have stronger daytime heat islands are classified as low data quality. While the summer and winter UHI magnitudes averaged for all cities is similar (1.04 ˚C winter, 0.97 ˚C summer) the heat islands of individual cities are highly variable between summer and winter; the average difference between summer and winter heat island for each city is 0.51 ˚C with 35 expressing a stronger summer UHI and 28 showing stronger winter UHIs. For cities classified as medium or high data quality, the summer and winter averages across all cities is higher, but similar between the two seasons (1.20 ˚C winter, 1.22 ˚C summer). The seasonal differences are stronger for the nighttime UHI than the daily average UHI. In Mexico City, the heat island increases from 1.98 ˚C in JJA to 4.89 ˚C in DJF.

3.1.2 Example heat islands

Figures 1 – 4 present some examples of urban heat islands that show the general behavior of the heat island and how it varies on a daily and annual basis. The examples

shown include the world's most populous city (Tokyo, Japan) as well as others that demonstrate some of the variability seen in heat islands.

3.1.2.1 Tokyo, Japan

The heat island of Tokyo, Japan reaches a maximum in the early morning, with an hourly average UHI of 3.7 ˚C (Fig. 3a). There is a strong transition in the UHI from nighttime to daytime as the January heat island magnitude decreases by 2.9 ˚C between 0700 and 1100 local time (LST) and the June UHI decreases by 1.7 ˚C between 0500 and 0900 local time. The timing of the shift between the strong nocturnal and weaker daytime heat island is related to the timing of sunrise and sunset and is a common feature of the heat island. The Tokyo heat island has the strongest daytime magnitude during the summer, with urban temperatures elevated by 0.93 ˚C at noon in June compared to 0.67 ˚C in December.

3.1.2.2 Phoenix, AZ

The Phoenix, AZ heat island (Fig. 3b), which has the highest annual average heat island magnitude, displays a similar diurnal pattern to Tokyo but the seasonal values approach a maximum in June with nighttime heat island magnitudes of up to 4.5 ˚C. The nighttime UHI in July is significantly lower than in June at the onset of the North American Monsoon, with the maximum nighttime value falling to 2.9 ˚C.

3.1.2.3 Paris, France

The Paris, France heat island (Fig. 3c) has lower maximum UHI values than Tokyo or Phoenix. Paris shows greater seasonal changes in the timing of the daily onset

and weakening of the nighttime heat island due to the increased day length in summer as a result of its high latitude (49˚N compared to 36˚N for Tokyo and 33˚N for Phoenix).

3.1.2.4 Recife, Brazil

Recife, a tropical city near the equator (8˚S), has a heat island (Fig. 3d) that differs from the others presented in that the seasonal cycle is dominated by the climatology of the precipitation rather than changes in temperature (the average temperature of the warmest and coolest months only differ by 1.4 ˚C.) The Recife wet season runs from April to July, which corresponds to the months with the lowest UHI magnitude with a peak UHI of 1.7 ˚C during July. As Recife enters the dry season the maximum UHI increases, reaching 3.1 ˚C by October. The shift to the urban stations being cooler than the rural stations during the daytime from September to March is a feature that appears in several cities along large water bodies. It is primarily present when the selected urban stations are closer to the water than the rural stations, indicating that the negative UHI may be a feature of the relative location of urban and rural stations rather than a true representation of the urban climate.

3.2 Controls on UHI development

3.2.1 Latitudinal Controls

The latitudinal position of a city has several influences on the development of the UHI. The summer nighttime heat island shows a strong positive response to total daily insolation (Fig. 4). The correlation between summer nighttime UHI magnitude and total daily insolation at the solstice for cities of medium and high data quality is 0.66 for all extratropical cities and 0.81 for temperate cities ($p < 0.001$ in both cases) which translates

to an R^2 of 0.44 and 0.66, respectively. However, the correlation between the average monthly UHI and average monthly insolation is not significantly different from zero. In the winter the influence of latitude on nighttime heat island magnitude is weaker, with only temperate cities demonstrating a significant correlation between the UHI and latitude (R = 0.23) or insolation (R=-0.23). The change in the relative magnitudes of the UHI between summer and winter also shows a latitudinal dependence, with all cities greater than 38˚ north or south demonstrating stronger summer time UHIs, while cities at lower latitudes do not show a consistent seasonal pattern in UHI magnitude (Figure 2).

The hourly rate of temperature change (i.e., the heating rate) for the urban and rural stations for each city provides additional information on how heat islands develop. The heating rate differential between the urban and rural areas is important for understanding heat island development because the periods where the differential is greatest are the periods when the magnitude of the heat island is growing or shrinking. For example, the differential heating rates for London, UK and Houston, TX show the importance of the time around sunrise and sunset to heat island development as these periods mark the timeframe when the heating rate for urban and rural regions strongly diverge from each other (Fig. 5). Aside from these periods the heating and cooling rates of the urban and rural stations are similar, leading to a relatively constant UHI. The greater seasonal shift in the timing of the onset of the nocturnal London heat island relative to that of Houston is the result of higher latitudes having a much greater shift in the timing of sunrise and sunset over the course of the year, leading to changes in the daily development of the heat island and the length of the nocturnal heat island.

Latitude also appears to display control over the relative strengths of the summer and winter heat islands for each city. At low latitudes the nighttime UHIs (Fig. 6) does not show a clear pattern as whether the winter (DJF in Northern Hemisphere, JJA in Southern Hemisphere) or summer (JJA north, DJF south) heat islands have the greatest magnitude. At latitudes greater than 38˚, all but two cities (Shenyang and Changchun, both of low quality) have stronger heat islands in summer than in winter.

3.2.2 Meteorological Controls

3.2.2.1 Wind Speed

Wind speed negatively correlates with heat island development, with calm winds more likely to affect the development of a strong heat island. Observations of nighttime UHI and wind speed for the Minneapolis - Saint Paul region (Fig. 7) show stronger heat island magnitudes at very low wind speeds and decreasing UHI up to about 5 m s^{-1}, above which the UHI does not vary with respect to wind speed. This nocturnal feature is present in both summer and winter although the magnitude differs, but is not present consistently during the daytime. This differential between calm and windy conditions is a consistent UHI feature, with most cities demonstrating stronger heat islands in low wind conditions during both summer and winter (Table 3).

3.2.2.2 Sky Cover

In general, cloudier conditions weaken heat island development. As an example, the average UHI magnitudes under clear/scattered skies versus overcast skies for Chicago, IL (Fig. 8) show that clear sky conditions lead to the development of a much stronger nocturnal heat island. This differential in the UHI between clear/scattered and

overcast conditions is a feature that is observed in the UHIs of most of the cities analyzed. Clear skies coincide with stronger heat islands in the vast majority of cities in both summer and winter (Table 3) while there are very few cities that demonstrate the opposite relationship.

3.2.2.3 Dew Point Temperature

Low humidity atmospheric conditions lead to a stronger heat island. This feature is observed in most of the cities examined, with only three low quality cities demonstrating the opposite trend during summer nights (Table 3). This feature also appears frequently during daytime periods when the UHI tends to be weaker and more variable, although in most cases the difference between humid and dry conditions is not strongly significant. On dry days during the summer, the heat island increased by over 1.0 ˚C in 15 cities relative to humid days. At night there were 37 cities with a 1.0 ˚C increase in the heat island with 10 cities having an increase of 2.0 ˚C. The winter also shows stronger UHIs with dry air, although there were fewer cities with significant differences between humid and dry conditions. Atlanta, GA is an example of this feature, with the summer nighttime heat island being inversely correlated with dewpoint temperature (Fig. 9a). This feature is even stronger when assessing the relationship between the UHI and dewpoint depression, with drier air leading to a large increase in the UHI (Fig. 9b) with a correlation of 0.63.

3.2.2.4 Temperature

The relationship between temperature and heat island development is significant with results indicating that excessive heat events lead to stronger heat island conditions.

Four times as many cities show stronger UHIs on summer nights when the overnight temperature was higher (more than one standard deviation above normal) than show a stronger UHI when the temperature was lower (one standard deviation below normal) (Table 3). This feature is different from the other meteorological influences on the UHI in that it appears stronger during the daytime rather than nighttime. The number of cities that show stronger UHIs in warm weather on summer days is nine times the number of cities that show stronger heat islands during cool periods, although half the cities (n=34) did not produce significant results. As an example, the New York City afternoon heat island response to temperature shows that increasing temperatures correspond to an increase in the heat island magnitude of over 1.5˚C between the hottest and coldest periods (Fig. 10). For New York City this feature is primarily a summertime and afternoon/early evening response (Fig. 11). During summer heat waves, the heat island increased by over 1.0 ˚C in 13 cities during the day and 21 at night, with 8 cities having an increase in the nocturnal heat island of over 2.0 ˚C. In winter the influence of temperature on the UHI is less clear as the cities are split between showing increased UHIs with high temperatures or low temperatures. The high quality cities, however, show a nighttime heat island that is stronger during cold periods; particularly as the winter average temperature decreases (Fig. 12). Of note is the fact that each of the seven Chinese cities in the study that show a significant warm/cold differential have an increased UHI during warmer periods, which is of an opposite trend to most of the cities in the study.

3.2.2.5 Precipitation

In tropical regions seasonality is most strongly defined by wet and dry seasons, which in turn influences heat island development. The correlation between a city's monthly average UHI and monthly average precipitation is strongly negative for most tropical cities (Fig. 13). The Mexico City monthly heat island and monthly precipitation across the study period shows this influence strongly with months that have less than 10 mm of precipitation having an average heat island of 4.6 ˚C while months with more than 10 mm of rain have an average heat island of 2.3 ˚C (Fig. 14). For cities outside the tropics, only the arid and Mediterranean climates demonstrate this correlation between precipitation and heat island magnitude. For cities in the temperate biome the seasonality shifts away from wet and dry seasons and this correlation breaks down as variability in solar energy received and temperature dominate (Fig. 13).

3.2.3 Environmental Factors

3.2.3.1 Population

The importance of population and population density of a city on heat island development is seasonally variable with the influence of population and population density on the wintertime heat island being strong. The correlation with UHI and the population is 0.56 for all cities, and 0.66 for cities in temperate biomes (Fig. 15). The correlation with population density for the innermost 10 km part of the city is only slightly lower at 0.52 and 0.62 respectively (Fig. 16). This was the strongest correlation of any of the environmental factors for the winter period and the range of fitted values from a regression of the population and the heat island magnitude is 2.2˚C. In the summer

period the influence of population shows a weakly significant correlation with the urban heat island magnitude (Table 4). However, this population trend may not be a true feature as the correlation is slightly negative without the city of Tokyo, which is an outlier because of its size and heat island.

3.2.3.2 Vegetation

The relationship between the summer monthly rural and urban NDVI and the UHI magnitude indicates that vegetation influences the heat island. For all extratropical cities, the rural NDVI does not show a significant correlation with the UHI magnitude, but for temperate cities the correlation is 0.30 (Table 3, Fig. 17) and increases to 0.37 when comparing the rural NDVI to the log of the UHI magnitude. The urban NDVI does not show a significant correlation with the UHI magnitude. The difference between the rural and urban NDVI is significantly correlated to the heat island magnitude for both extratropical cities (0.34) and temperate cities (0.39) (Fig. 18). The range of values from a regression of the UHI magnitude and the NDVI difference is 1.5˚C. Like the rural NDVI this trend becomes stronger when correlating with the log of the heat island magnitude (0.40 and 0.47 respectively).

3.2.3.3 Impervious Surfaces

The impervious surface fraction of cities significantly contributes to the formation of UHIs in both summer and winter. During summer nights the impervious fraction has a significant positive correlation with the UHI for all cities (0.30) and just temperate cities (0.36). The range of the regression fit between UHI and the impervious surface fraction for all cities is 1.0 ˚C and 1.1˚C for only temperate cities (Fig. 19). In winter, the

impervious fraction more strongly correlates with the heat island (0.36 for all cities) (Fig. 20) with a range in the regression fit of 1.1˚C.

3.2.3.4 Air Pollution

Air pollution shows a significant negative correlation with the summer heat island. In the summer all cities show a negative trend in the UHI with increasing PM10 pollution that is even stronger for cities in the temperate biome (Table 4). Regression of air pollution with the UHI leads to a range of the fitted result of 1.52 ˚C (Fig. 21). In winter the correlation between the UHI and air pollutions is not significant. This relationship is also apparent in the full data set that includes all cities as 11 of 13 of the cities in the highest quartile of air pollution in the highest quartile had UHI's below the mean for all cities.

3.2.3.5 Combination of Environmental Factors

The correlations between individual variables and the UHI during the summer show that several factors have a significant relationship with the heat island of cities. This suggests that analysis of multiple variables in combination can likely explain a greater fraction of the variability in the UHI than any single environmental factor. Multiple linear regression of the environmental factors against the UHI and log of the UHI for temperate cities shows that some combinations provide increased predictive capacity for the magnitude of the heat island (Table 5). In particular the combination of rural vegetation, air pollution and population density can explain 44% of the variability in the log of the UHI. In two environmental factor combinations, the urban-rural NDVI difference pairings shows stronger correlations and larger fit ranges than the rural vegetation

pairings, but rural NDVI becomes stronger in three environmental factor groupings because it is more independent of the other variables (i.e., the NDVI difference has a stronger correlation with pollution, population and impervious surface factors).

Chapter 4

Discussion

The uniqueness of this study is in the analysis of the urban heat island behavior of 64 cities around the globe that represent a variety of geographic regions with disparate climates and biomes. This methodology allows for an analysis of the many factors that influence urban warming and provides the ability to compare the heat island behavior of multiple cities to find commonalities in the heat islands, to identify new heat island drivers, or to support previously reported behaviors. This analysis provides the opportunity to explore the variability of the heat island between cities and investigate the landscapes of those cities to determine which environmental factors are driving changes in heat island behavior. Ultimately, this information could be useful to urban practitioners who are tasked with reducing urban warming.

Atmospheric water vapor acts a strong control on heat island formation. Lower dewpoint temperatures and higher dewpoint depressions drive a strong heat island that is present during both daytime and nighttime periods, particularly during the summertime. Contrary to most other drivers, this driver is apparent during the daytime. There are several possible mechanisms that could contribute to a strong UHI on dry days. First, changes in the dewpoint depression correspond with changes in the vapor pressure deficit that can alter the latent heat flux in rural areas. On drier days the increased vapor pressure deficit will cause the vegetation to transpire more moisture, increasing the latent cooling effect and reducing rural temperatures. This cooling effect is reduced in urban areas due to a lower vegetation fraction relative to the surrounding rural landscape, thus strengthening the heat island. This mechanism is most responsible for the daytime UHI signal, as this rural cooling would result from daytime photosynthetic activity. Second,

high humidity can cause aerosols to swell and increase the radiation scattering effect (Jacob 1999), which increases the attenuation effect of air pollution in urban areas. This results in a decrease in solar radiation absorbed at the surface, which lowers the heat island magnitude relative to drier days. Extended periods of dry weather may also lead to drought or near-drought conditions when the rural surface energy balance exhibits behavior similar to that of tropical locations during the dry season. The low soil moisture has been shown to lead to a stronger UHI due to reduced heat capacity allowing greater nocturnal cooling of rural areas (Jauregui 1997). The drivers of the relationship between the UHI and the dewpoint depression are likely a combination of the above factors, and further analysis is needed to properly separate the individual contributions.

This analysis also contributed to identifying another important driver of urban heat island behavior – heat waves. That is, the heat island is strongest during hot weather when it can be most detrimental to urban residents. The relationship between the heat island and heat waves has a few possible mechanisms that could explain the observed behavior. During heat wave events the high temperatures lead to larger dewpoint depressions because the dewpoint temperature does not increase as much as the temperature. All of the cities analyzed show a larger average dewpoint depression during heat waves than during cold air outbreaks. This implies that the mechanisms that increase the heat island in dry conditions are also active during heat waves. The latent cooling of rural areas can be particularly strong during heat waves because the nonlinear relationship of saturation vapor pressure and temperature leads to very large vapor pressure deficits at high temperatures. Increased rejection of waste heat from buildings

due to greater air conditioning demand during heat waves can also contribute to a stronger heat island. Models have projected that during heat waves air conditioning could raise the heat island magnitude in urban cores by 0.5 – 1.0 ˚C (Salamanca et al. 2014; Tremeac et al. 2012).

Tropical cities and extratropical cities with dry summers show a common response that indicates the importance of seasonal precipitation on the heat island. Cities with a seasonality that is primarily defined by wet and dry seasons have the strongest heat islands during the dry seasons. This behavior indicates that planning policies designed to reduce the heat island might differ among cities as a function of seasonal precipitation. Previous studies showed that Mexico City, Mexico had a strong dry season heat island due to low seasonal soil moisture resulting in low rural heat capacity and more efficient nighttime rural cooling (Jauregui 1997). The results presented here indicate that this mechanism could extend to most tropical cities. This behavior was also found outside the tropics in the Mediterranean and arid climate cities during the summer months, implying that the same mechanism functions in the urban regions of these climates. These cities showed much weaker correlations with urban environmental factors, particularly NDVI, than did cities in temperate vegetated regions, thus indicating that different surface energy mechanisms are influencing the heat island in these dry cities versus temperate cities. Phoenix, AZ provides an excellent example, as the month of June is very dry (<4 mm of rain on average) and has the strongest nocturnal heat island (4.3 ˚C), after which the North American Monsoon sets in during July (21 mm of precipitation) and the heat island magnitude drops to 3.0 ˚C in July and 3.1 ˚C in August. The other cities in the arid

and Mediterranean climates have lower seasonal precipitation than Phoenix and the dryness of these cities explains why these heat islands behave differently in summer as compared to the temperate cities. Because cities with strong dry seasons have the greatest UHI during periods of vegetative inactivity, mitigation should focus on the urban form (i.e., gray infrastructure) rather than land use change efforts intended to increase urban greenness (e.g., urban tree planting).

In addition to these new results, the commonalities seen in the heat islands studied confirmed the findings of numerous studies that have examined the factors contributing to urban heat island development. These results support previous work showing that the differences in heating and cooling rates between urban and rural areas peak around sunrise and sunset, and this behavior drives the development of a strong nocturnal heat island. The previously reported behavior of the heat island becoming much stronger as cloud cover and wind speed decrease is also found in almost all of the cities studied.

This analysis of the relationship between the summer and winter heat islands of cities addresses a discrepancy in the urban heat island literature. With the analysis of many cities, a pattern emerges in the seasonal heat island behavior between high and low latitudes. At high latitudes (above 40˚ N) all of the cities demonstrated stronger heat islands during the summer months than in winter, while at lower latitudes the results become scattered, with no clear trend in the season with the strongest heat island (Fig. 4). Souch and Grimmond (2006) concluded that the heat island was stronger in winter while Arnfield (2003) found the opposite result. This discrepancy resulted from a combination of using a small sample of cities and the particular location of the cities that were

evaluated. Souch and Grimmond included mostly lower latitude cities while Arnfield considered more northern cities. Because both studies selected only a few cities in assessing the seasonal influence of the heat island they did not have enough data to identify the variability below 40 ˚N/S and with a small sample could find cities that allowed for contradicting conclusions.

The latitudinal nature of the seasonal heat island behavior is the result of differences in surface energy availability in the summer and winter. At the higher latitudes the differential in total daily insolation between the summer and winter is substantial—the seasonal average daily insolation is over three times greater in summer than in winter at 45˚ N/S. Because the heat island is driven by variations in the surface energy balance between urban and rural areas, decreases in absorbed radiation limit the total energy available to drive a strong urban-rural differential. This means that cities at high latitudes can develop stronger heat islands in summer than in winter.

The relationship between the heat island and vegetation illustrates the importance of vegetation in the development of the heat island and presents an opportunity for mitigation. The negative correlation between NDVI and the UHI for temperate cities provides evidence that greater rural vegetation, and thus latent cooling, strengthens the heat island. The large variability about the regression line of the NDVI and UHI (Fig. 18b) is a function of other factors contributing to the behavior of the heat island for individual cities - the largest deviations are cities like Tokyo (the most populous, densest city) and Hangzhou (greatest air pollution). The difference in NDVI between urban and rural regions more strongly correlates with the heat island magnitude than the rural NDVI

does alone, indicating that the urban vegetation is also influencing the heat island. Smaller differences between urban and rural vegetation result in a weaker summertime heat island due to less substantial changes in the vegetative contribution to the surface energy balance. As a result, urban design that increases urban vegetation coverage could provide some mitigation of the heat island.

The impervious surface fraction has a significant and substantial correlation with the heat island, indicating that the changes to the urban surface are driving increases in sensible heating. These changes function to increase daytime heat storage in the urban surface and drive a stronger heat island. The impervious surface measurements also reflect denser urban canyons, with reduced sky view factors, leading to changes in the radiation balance from reduced long wave emissions out of the canopy and decreased albedo that function to strengthen the heat island. This indicates that alterations to the urban form (materials and geometry) can also help mitigate the heat island.

Cities could see increases in the heat island as a side effect of efforts to limit air pollution, which could result in urban temperature increases of over a 1˚ C in the most heavily polluted cities. The relatively weak heat islands seen in cities with high air pollution relative to cities with cleaner air is evidence that the reductions in downward shortwave radiation caused by air pollution can play a significant mitigating role in the development of the heat island. The correlation and regression results of the UHI with large particulate pollution show that this mechanism can substantially weaken the heat island of heavily polluted cities, with the regression indicating that the result of air pollution in the most heavily polluted cities is a reduction in air temperatures of 1.5 ˚C.

The strong reduction in UHI from the pollution also indicates that the reduced downward shortwave radiation greatly exceeds any longwave trapping effect from a polluted layer with a greater longwave emissivity.

In the winter the behavior of the heat island provides evidence that anthropogenic energy substantially influences the heat island. In extratropical cities, the winter UHI is strongly correlated with population and population density with more populous cities exhibiting much stronger heat islands. While this could be an indication of the influence of urban geometry and materials, the correlations of population and density with heat island magnitude are much stronger than the impervious surface fraction's correlation with the heat island. This indicates that the winter heat island is strongly defined by population-specific causes rather than the urban form, implying that anthropogenic energy use is a significant factor in the heat island in the winter heat island. This result also matches modeling studies that have indicated that anthropogenic heat can contribute over 2 ˚C to the winter nocturnal heat island (Fan; Sailor 2005; Ichinose et al. 1999). Additionally, the winter anthropogenic heat comprises a significant fraction of the energy available at the surface, unlike in summer, allowing it to contribute to relative differences in the surface energy balance between urban and rural areas. Of the eleven cities where the average winter temperature was below -1.5 ˚C, nine displayed a stronger nocturnal heat island during extreme cold events than when the temperature was above average (the two opposing cities were the low data quality cities of Shenyang and Changchun.) This increase in the heat island as temperature decreases and heating demand and energy usage grows is evidence that anthropogenic energy strengthens the heat island and is

supported by findings that in cold weather cities use more substantially energy at night than other cities (Sailor; Hart 2006). Population strongly contributes to the heat island in winter while only weakly affecting it during the summer. This finding provides some useful guidance for large, high latitude cities, implying that controllable factors like urban form and vegetation are available to mitigate the summer heat island, even in the largest cities.

Chapter 5

Conclusions

5.1 Summary

In this study, the urban heat island behavior of 64 cities around the world was analyzed in a manner that is markedly different from past studies, which have tended to focus on the heat islands of individual cities or small groups of cities. This approach allows the comparison of a large sample of cities to identify common behavior in the heat island and to investigate the driving forces behind the variability between cities. With this approach, new aspects of the heat island were identified and the relative strengths of various environmental factors that influence the heat island were quantified. Additionally, many of the results from the study are in agreement with the findings of individual city studies, confirming these features as general heat island behavior. Two unique features of heat islands were identified - in dry weather and during heat waves cities showed stronger heat islands, with increases of up to 1.0 ˚C during the day and 2.0˚C at night, relative to more humid or cooler periods. Changes to the heat island were also analyzed as urban environmental factors vary among cities, providing estimates of how those features can alter the strength of the heat island. Temperate cities with the greatest difference between urban and rural vegetation have heat islands that can be over 1.0 ˚C stronger than cities where the vegetation differential is smaller. Very high impervious surface fractions increase the heat island in summer by up to 1.0 ˚C relative to more sparsely developed cities. Air pollution mitigates the heat island, with the most heavily polluted cities seeing a decrease in the heat island magnitude of up to 1.5 ˚C. In the winter the more populous cities showed significantly stronger heat islands (up to 2.0 ˚C for Tokyo) than the

relatively smaller cities, yet there was little relationship between population or population density and urban heat island in summer.

These results reveal several important heat island traits that can inform urban practitioners as to how best to mitigate urban warming. Most important is the finding that during heat waves the urban heat island is stronger than normal. Because the biggest threat to the urban population from heat islands is increased heat stress and mortality, this means the urban plans for dealing with heat waves need to expect urban core temperatures that may be even higher than anticipated and heat stress on the population will need to be aggressively managed. Because part of this temperature increase is the result of heat rejection from building air conditioning, methods of keeping buildings cool that do not reject the excess heat into the urban atmosphere (i.e. white roofs, thermal storage systems) would help to mitigate this driver. Increasing urban vegetation is a method that can be used to limit urban temperature increases through latent cooling, although changes in heat indices may be more limited as this would increase local dewpoint temperatures. Intelligent alterations of city structure can also play a role in minimizing the heat island. Cities in vegetated regions show strong responses to both infrastructure and vegetation, indicating that efforts to influence the nature of the gray infrastructure and the amount of urban vegetation can limit the summertime heat island. For cities with strong dry seasons the results demonstrated that the heat island is strongest during the dry season when vegetative activity is low, indicating that heat island mitigation efforts should primarily involve the gray infrastructure, focusing on the surface materials, albedo and canyon geometry. The influence of population and

population density on the heat island was substantially weaker than other factors in the summer, indicating that cities with very large populations have methods available to reduce urban warming. In the winter the population relationship to the heat island is much stronger, which may actually be beneficial to large cities in cold climates. One factor that is a potential difficulty for urban planners is the relationship between air pollution and the heat island, as efforts to reduce air pollution could have the side effect of increasing the heat island.

5.2 Future Work

This research suggests avenues for future investigations into urban heat islands as a number of the results shown here provide general ideas of which factors influence the urban heat island. Studies directed to particular variables could provide a better understanding of the mechanisms behind the observed behavior. The dewpoint depression and heat wave results are new and merit further analysis, which could help in developing appropriate mitigation strategies for the heat island. The estimates of how strongly environmental features drive changes in the heat island could be better constrained by studies using a smaller group of cities.

While the heat wave and dewpoint temperature results are new, investigations on smaller scales with individual cities could aid in comprehension of the mechanisms behind these phenomena. Studies of the energy balances of individual cities have been performed in the past, and similar methods could be used to measure changes in the energy balance as the humidity changes. This methodology can provide for a more comprehensive analysis of the changes in surface energy partitioning between the urban

core and surrounding rural regions to determine if changes in latent cooling explain the difference in heat island behavior between dry and humid days. An energy balance study could also be performed to investigate the heat wave behavior, and the influence of latent cooling on the heat island should be detectable in the same manner. Assessing the contribution of building cooling is more difficult as building heat rejection is both a function of an increase in anthropogenic heat as energy usage to drive cooling demands increase with temperature, and a reduction in the surface energy storage (i.e., heat within buildings is effectively part of the surface storage term). In a study of a single city, energy utilities may be able to provide more detailed assessments of energy usage on smaller scales to allow for an accurate estimate of the anthropogenic heat loss during heat waves. This should provide a more accurate closing of the energy balance by better quantifying the surface storage term. Changes to the surface storage term and anthropogenic heat relative to cooler periods should provide some insight into the influence of the air conditioning of buildings on the magnitude of the heat island.

Better assessment of the energy usage within cities could also help in quantifying the influence of anthropogenic heat on the heat island, particularly in winter. Anthropogenic energy usage in some countries has been documented fairly well, but in many others the data for individual cities is limited. The influence of air pollution on urban temperatures can also be better constrained in smaller studies that can obtain daily pollution values to compare with daily measurements of the heat island. The impervious surface data used to assess the impact of the built environment on the heat island represents several of the mechanisms that are changed in the surface energy budget of the

surface. Studies that can separate these behaviors can provide better insight into the heat island. Albedo changes, longwave energy trapping and ground storage of heat during the daytime are all captured in the impervious surface area metric and separating these factors could help in assessing the individual mechanisms responsible for urban warming. In particular, the albedo is an urban factor that can be managed by urban planning (i.e. white roofs) but it was not assessed in this study due to sparse values of satellite-sensed albedo for many of the cities. Quality albedo assessments, particularly if they account for albedo changes with sun angle would help in understanding the strengths of the individual mechanisms of the built environment that influence the heat island.

This study demonstrates that while the urban heat island is a feature of cities that can increase risks for urban populations, mechanisms are available for urban planners to reduce the warming and mitigate these risks. The behavior of the heat island as vegetation and impervious surface area vary between cities indicates that the heat island is responsive to changes in the urban landscape. As a result, increases in urban vegetation and changes to the makeup of the built environment that reduce the energy at the surface are actions that can be taken to mitigate urban warming. Continued investigation into the urban heat island along the paths recommended here would permit better assessment of the risks of the urban heat island and allow for more specific option to control urban temperatures.

Tables

	Condition A	Condition B
Wind	Low Winds (≤ 3 m s^{-1})	High Winds (≥ 5 m s^{-1})
Sky Cover	Clear/Scattered	Overcast
Temperature	Warm ($\geq$ 1 st. dev. above average temp)	Cool ($\leq$ 1 st. dev. below average temp)
Dewpoint Depression	Dry (depression $\geq$ .75 above average)	Humid (depression $\leq$ .75 below average)

Table 1. Categories for assessing the UHI under contrasting meteorological conditions.

City	UHI (˚C)							Biome	Data Quality
	Annual	Winter	Summer	Day	Night	Winter Night	Summer Night		
Ankara, Turkey	1.16	1.30	1.32	0.82	1.39	1.35	1.79	Temperate	Low
Athens, Greece	2.06	2.23	**2.10**	1.51	2.68	2.48	**3.22**	Mediterranean	Med
Atlanta, USA	0.83	0.60	0.93	0.00	1.44	1.02	1.65	Temperate	High
Baghdad, Iraq	0.21	0.09	0.36	-0.22	0.55	0.22	0.78	Arid	Low
Bangalore, India	0.47	1.19	-0.29	0.02	0.94	1.99	-0.13	Tropical	Low
Bangkok, Thailand	0.83	1.03	0.78	0.02	1.34	1.88	1.09	Tropical	High
Barcelona, Spain	1.16	1.45	0.85	-0.95	2.68	2.51	2.98	Mediterranean	Low
Beunos Aires, Argentina	0.93	1.18	0.50	-0.73	2.32	2.14	2.29	Temperate	High
Boston, USA	0.74	0.35	0.92	-0.42	1.66	0.80	2.16	Temperate	High
Cape Town, South Africa	-0.09	0.16	-0.17	-1.01	0.72	0.63	0.95	Mediterranean	Low
Changchun, China	0.60	1.35	-0.06	0.13	1.03	2.08	0.25	Temperate	Low
Chengdu, China	0.90	0.86	0.92	0.72	1.04	1.04	1.04	Temperate	Low
Chicago, USA	1.18	1.23	1.24	0.25	1.93	1.47	2.38	Temperate	High
Chonqing, China	1.23	1.33	1.36	1.17	1.38	1.56	1.38	Temperate	Low
Dallas, USA	1.05	1.00	1.03	0.32	1.66	1.46	1.79	Temperate	High
Detroit, USA	1.07	0.67	1.46	0.47	1.61	0.82	2.49	Temperate	High
Dhaka, Bangladesh	1.29	1.71	0.93	0.22	2.15	3.06	1.40	Temperate	Med
Hangzhou, China	0.53	0.64	0.38	0.26	0.78	0.89	0.50	Temperate	Med
Houston, USA	0.82	0.71	0.81	0.32	1.22	1.05	1.21	Temperate	High
Istanbul, Turkey	1.14	1.24	1.38	-0.74	2.48	1.98	*3.39*	Temperate	Low
Jakarta, Indonesia	1.34	1.58	0.96	0.78	1.91	2.28	1.34	Tropical	High

Johannesburg, South Africa	-0.26	0.77	-1.08	-1.78	0.90	2.23	-0.27	Temperate	Low
Khartoum, Sudan	1.16	-0.39	*2.65*	0.19	1.95	0.48	3.18	Tropical	Low
Kiev, Ukraine	0.72	0.63	0.70	-0.03	1.45	0.75	1.91	Temperate	Low
Kunming, China	0.96	1.66	0.47	0.91	1.04	1.51	0.71	Temperate	Low
Lisbon, Portugal	0.82	0.28	1.51	0.67	0.96	0.44	1.56	Mediterranean	High
London, UK	1.15	1.14	1.21	0.64	1.85	1.38	2.36	Temperate	High
Los Angeles, USA	1.99	1.77	1.98	1.13	2.70	2.53	2.47	Mediterranean	High
Madrid, Spain	0.67	0.52	0.88	0.22	1.07	0.77	1.49	Mediterranean	Low
Manila, Philippines	0.48	0.21	0.71	-0.04	0.93	0.85	0.91	Tropical	Med
Melbourne, Australia	1.86	1.52	2.04	**1.16**	2.35	1.76	2.79	Temperate	High
Mexico City, Mexico	1.94	**2.42**	1.54	0.43	**3.54**	**4.89**	1.98	Tropical	Med
Miami, USA	0.52	0.56	0.47	0.32	0.64	0.67	0.61	Temperate	High
Minneapolis - Saint Paul, USA	1.28	0.90	1.77	0.65	1.80	1.16	2.60	Temperate	High
Minsk, Belorus	0.67	0.64	0.69	0.22	1.49	0.78	2.17	Temperate	Med
Montreal, Canada	0.88	0.71	0.98	-0.12	1.71	1.09	2.19	Temperate	High
Moscow, Russia	0.51	0.66	0.49	-0.02	0.96	0.78	1.33	Temperate	Low
Nairobi, Kenya	0.58	0.16	0.86	-0.11	0.90	-0.13	1.76	Tropical	Med
New York City, USA	1.38	1.17	1.68	0.63	1.94	1.47	2.47	Temperate	High
Osaka-Kobe, Japan	1.84	1.95	1.42	0.63	2.83	2.69	2.44	Temperate	High
Paris, France	1.31	1.22	1.36	0.58	1.94	1.48	2.28	Temperate	High
Philadelphia, USA	1.72	1.51	2.00	0.97	2.26	1.80	2.80	Temperate	High
Porto Alegre, Brazil	1.06	1.23	0.76	0.97	0.91	0.98	-0.06	Temperate	Low
Phoenix, USA	**2.14**	2.15	1.89	0.75	3.30	2.79	3.14	Arid	High
Qingdao, China	0.46	1.18	-0.39	-0.66	1.35	2.09	0.12	Temperate	Low
Recife, Brazil	1.37	1.36	1.22	0.00	2.43	1.89	2.55	Tropical	Med

Rio de Janeiro, Brazil	0.50	0.40	0.45	0.05	0.80	0.81	0.79	Tropical	Med
Riyadh, Saudi Arabia	1.14	1.07	1.12	0.31	1.91	1.59	2.17	Arid	Low
Saint Petersburg, Russia	0.66	0.60	0.69	0.26	1.01	0.69	1.23	Temperate	Low
Sao Paolo, Brazil	-0.39	-0.06	-0.20	-1.59	0.71	1.12	0.69	Temperate	Low
Seattle, USA	1.21	1.47	0.93	0.02	2.10	1.75	2.42	Temperate	High
Seoul, South Korea	1.47	1.91	0.87	0.03	2.54	3.03	1.62	Temperate	High
Shanghai, China	1.34	1.68	1.01	1.01	1.62	1.86	1.23	Temperate	High
Shenyang, China	0.45	0.63	0.19	0.59	0.29	0.25	0.23	Temperate	Low
Shenzhen, China	0.99	0.91	0.96	0.25	1.43	1.31	1.58	Tropical	Med
Singapore, Singapore	1.42	1.01	1.69	0.36	2.10	1.27	2.67	Tropical	High
Sydney, Australia	1.15	1.01	1.20	0.81	1.22	0.85	1.54	Temperate	Med
Tehran, Iran	1.99	2.30	1.70	0.60	2.62	2.82	2.43	Arid	Med
Tokyo, Japan	2.03	2.33	2.01	0.86	2.92	3.34	2.85	Temperate	High
Toronto, Canada	1.45	1.75	1.44	0.66	2.13	1.92	2.44	Temperate	High
Warsaw, Poland	0.33	0.25	0.41	0.06	0.59	0.28	0.95	Temperate	Low
Washington, USA	0.92	0.59	1.19	-0.08	1.67	1.02	2.09	Temperate	High
Wuhan, China	0.46	0.19	0.70	0.16	0.69	0.32	1.03	Temperate	Low
Yangon, Myanmar	0.37	0.95	-0.15	0.13	0.68	1.79	-0.20	Tropical	Low

Table 2. The average UHI (˚C) for each city on annual, winter (DJF in the Northern Hemisphere, JJA south), summer (JJA north, DJF south), daytime (1100 to 1600 local time), nighttime (2300-0400), summer night and winter night time periods. Maximum UHI for medium or high data quality cities for each column in bold. Low quality extremes greater than the higher quality maximum in italics.

	Winter			**Summer**		
	Positive Sig	Negative Sig	Not Sig	Positive Sig	Negative Sig	Not Sig
Temperature (Cold periods – warm periods)				Cold: Temperature < 1 SD below normal Warm: > 1 SD above normal		
	Night					
All	20	26	18	9	36	19
HQ	15	6	7	5	13	10
MQ	1	5	6	1	8	3
LQ	4	15	5	3	15	6
	Day					
All	12	23	29	3	27	34
HQ	6	10	12	2	14	12
MQ	2	3	7	0	4	8
LQ	4	10	10	1	9	14
Sky cover (Clear or scattered – overcast)						
	Night					
All	47	5	12	42	2	20
HQ	24	1	3	24	0	4
MQ	9	0	3	9	1	2
LQ	14	4	6	9	1	14
Wind (Low winds - High winds)				Low: <3m/s High: >5m/s		
	Night					
All	37	7	20	37	10	17
HQ	24	0	4	25	2	1
MQ	4	3	5	7	0	5
LQ	9	4	11	5	8	11
Dewpoint Depression (Humid - Dry)				Dry: Dewpoint depression < .75 SD below normal. Humid: > .75 SD above normal		
	Night					
All	6	36	22	3	50	11
HQ	6	9	13	0	25	3
MQ	0	8	4	0	8	4
LQ	0	19	5	3	17	4
	Day					
All	6	26	32	5	23	36
HQ	4	13	11	2	11	15
MQ	1	3	8	1	4	7
LQ	1	10	13	2	8	14

Table 3. The number of cities with a significant difference ($p < 0.01$) in the mean UHI for the two meteorological conditions. Positive and negative UHI differentials are defined by the convention listed for each category. For temperature and dewpoint depression, the periods are limited to only those time periods where the sky cover was clear or scattered and the winds were less than 5 m/s.

	All Extratropical Cities		Temperate Cities	
	Summer	Winter	Summer	Winter
Latitude	0.52**	0.11	0.63**	0.23*
Insolation (Solstice)	0.66**	-0.12	0.81**	-0.23*
Insolation (Average)	-0.13	-0.06	-0.11	-0.14
Population	0.24**	0.54**	0.20*	0.64**
Population density	0.18*	0.47**	0.20*	0.58**
Impervious surface fraction	0.30**	0.36**	0.36**	0.43**
Rural NDVI	0.14	---	0.30**	---
Urban NDVI	-0.14	---	-0.18	---
NDVI Difference	0.34**	---	0.39**	---
Air Pollution (PM10)	-0.32**	-0.11	-0.43**	-0.01

Table 4. Correlation of UHI with environmental factors between cities. Correlations are calculated using medium and high quality cities for summer/winter nighttime UHI with clear/scattered skies and low winds. Data in presented for all extratropical cities and separately for temperate extratropical cities. * significant at $p > 0.1$ ** significant at $p > 0.05$

Two Factor Regression			R^2	UHI Fit Range
Rural NDVI	PM10		0.206	1.71
Rural NDVI	Impervious %		0.223	2.00
NDVI Diff	PM10		0.234	2.04
NDVI Diff	Population		0.201	1.74
NDVI Diff	Impervious %		0.249	2.03
PM10	Population		0.300	2.85
PM10	Pop. Density		0.343	2.66
PM10	Impervious %		0.294	2.16
Three Factor Regression				
Rural NDVI	PM10	Population	0.350	3.04
Rural NDVI	PM10	Pop. Density	0.374	2.69
Rural NDVI	PM10	Impervious %	0.323	2.36
NDVI Diff	PM10	Population	0.333	2.86
NDVI Diff	PM10	Pop. Density	0.353	2.62
NDVI Diff	PM10	Impervious %	0.328	2.42
PM10	Population	Impervious %	0.330	2.87
PM10	Pop. Density	Impervious %	0.363	2.79
Two Factor Regression against log(UHI)				
Rural NDVI	PM10		0.263	1.90
NDVI Diff	PM10		0.300	2.36
PM10	Population		0.306	3.23
PM10	Pop. Density		0.383	2.88
Three Factor Regression against log(UHI)				
Rural NDVI	PM10	Pop. Density	0.443	2.82
NDVI Diff	PM10	Pop. Density	0.417	2.56
PM10	Pop. Density	Impervious %	0.394	3.03

Table 5. Summer multiple variable regressions of environmental factors to UHI in temperate cities. The R^2 and the range of fitted values from the regression show the amount of influence the different variable combinations have on the UHI.

Figures

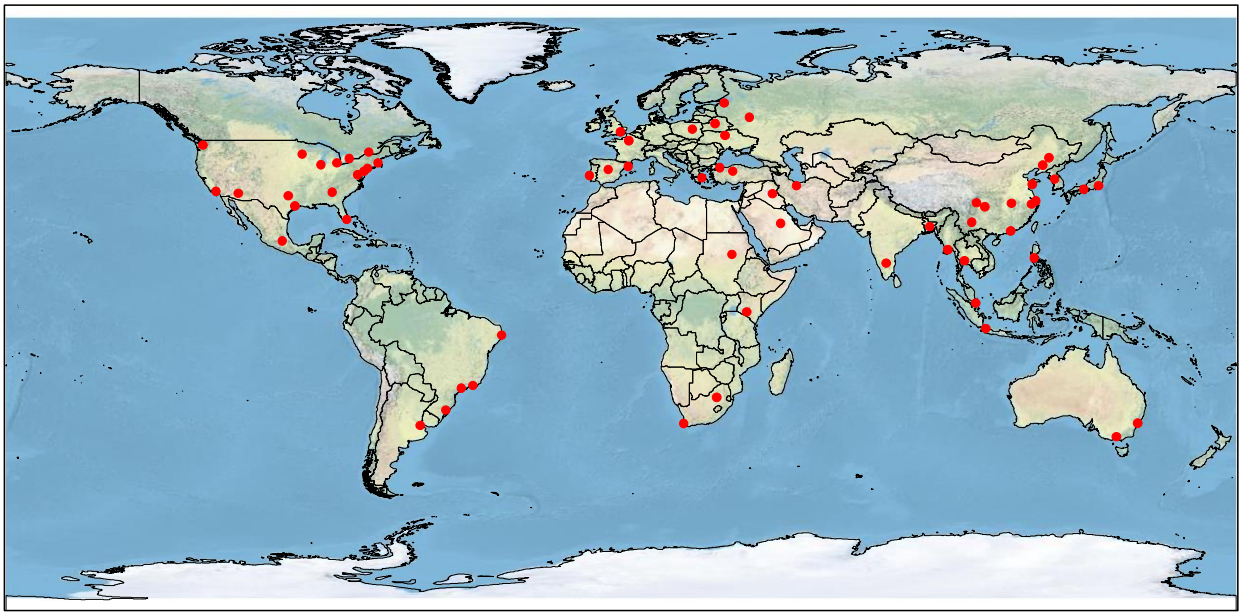

Figure 1. Cities in study

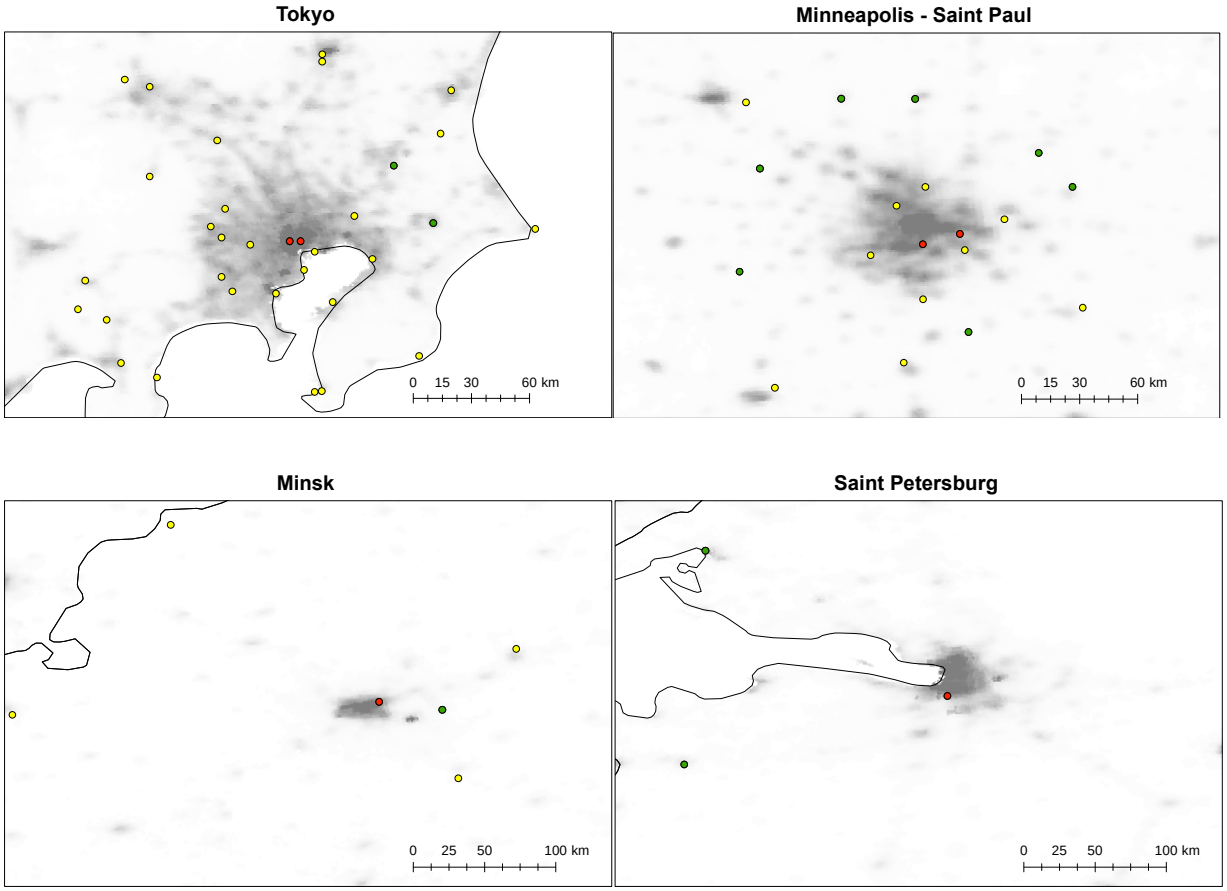

Figure 2. Station classification examples
Site locations for high data quality cities Tokyo, Japan and Minneapolis – Saint Paul, MN, medium data quality city Minsk, Belorus, and low data quality city Saint Petersburg, Russia. Red markers are stations used as urban sites, green are stations used for rural sites, and yellow markers are unused stations.

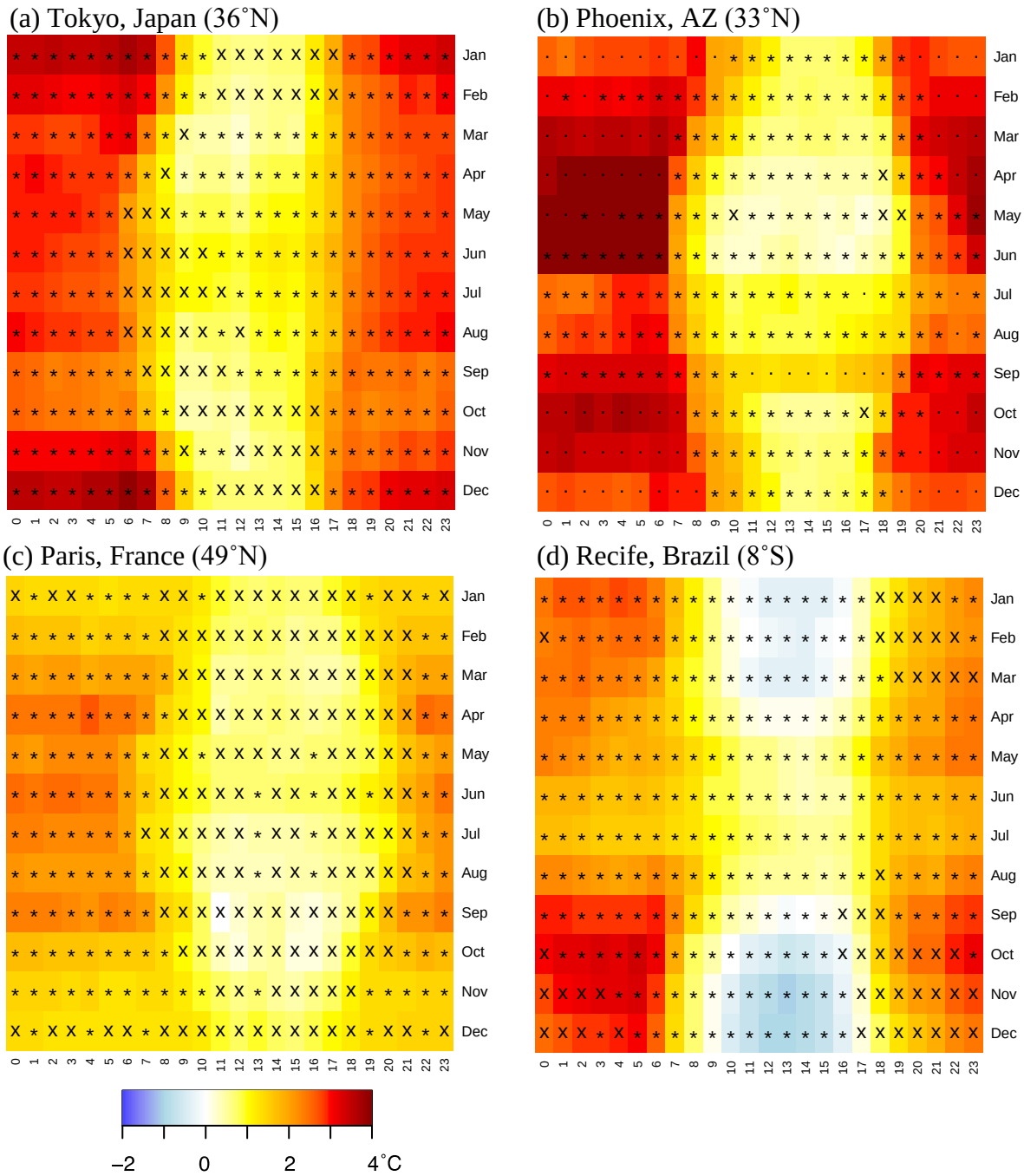

Figure 3. Heat island temporal maps for selected cities
The urban heat island magnitude for select cities plotted by month and hour of day (local time). Marks in each month hour point represent the width of the 95% confidence interval in the UHI magnitude: (.) ± 0.5 ˚C (*) ±0.25 ˚C (X) .125 ˚C

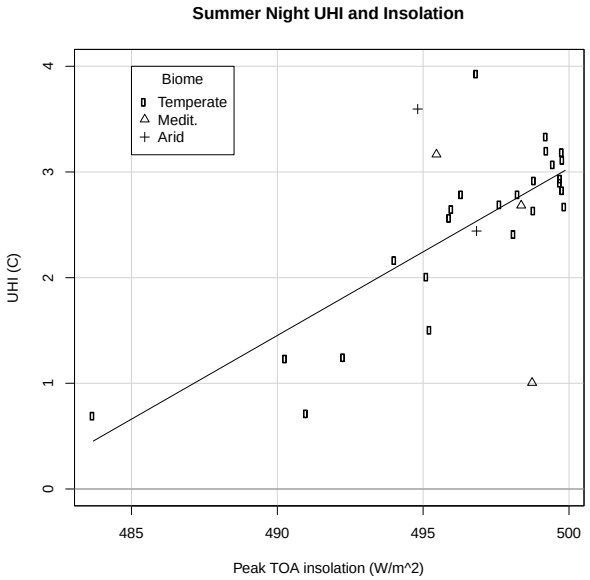

Figure 4. Summer UHI and insolation by city
Average summer nighttime UHI of extratropical cities and 24 hour average top of atmosphere insolation at summer solstice, grouped by biome with linear regression trend for all cities.

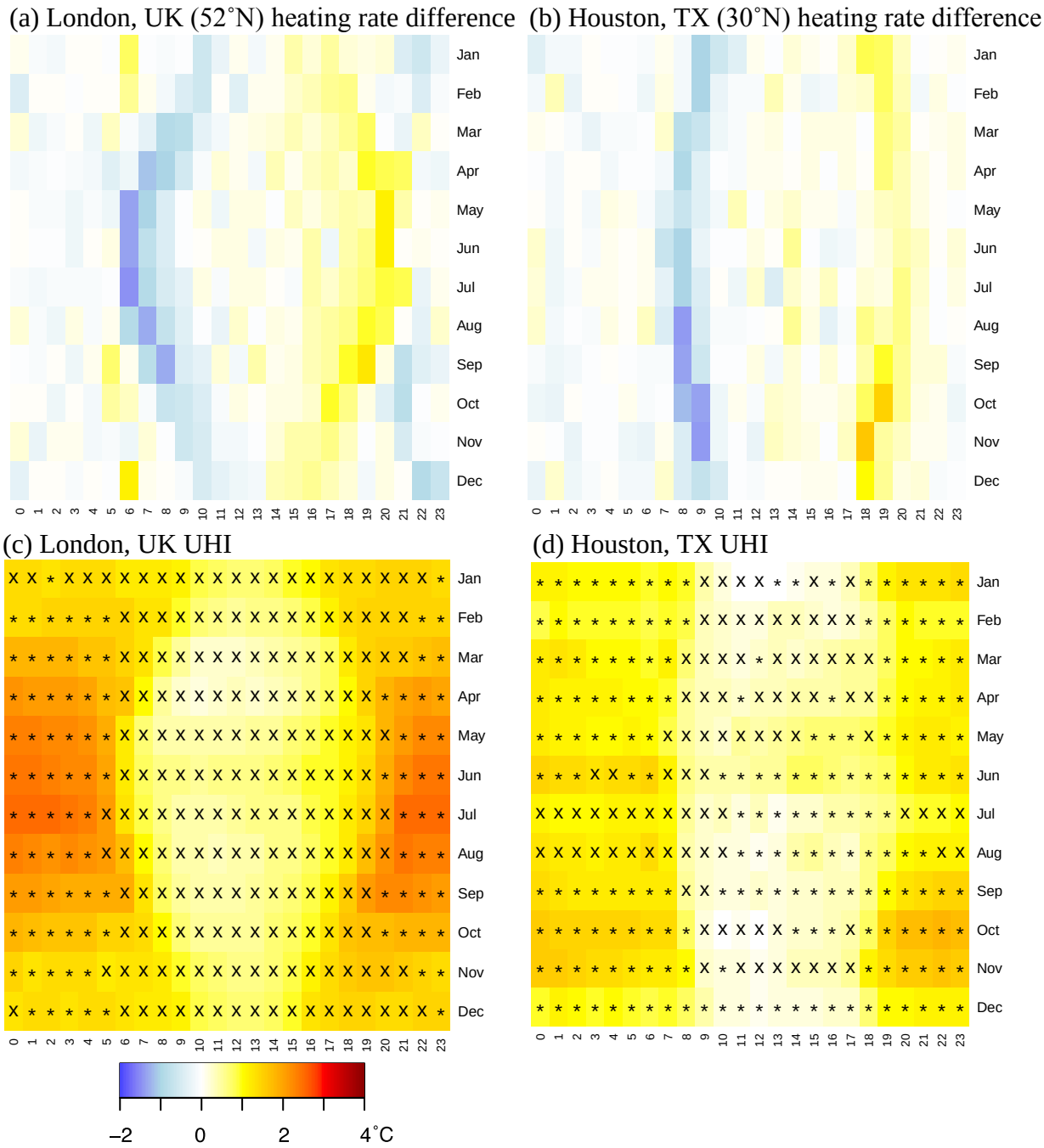

Figure 5. Heating rate and UHI development
Differential heating rate (urban – rural) for (a) London, UK (52˚N) and (b) Houston, TX (30˚N). UHI magnitude by month and hour for (c) London and (d) Houston.

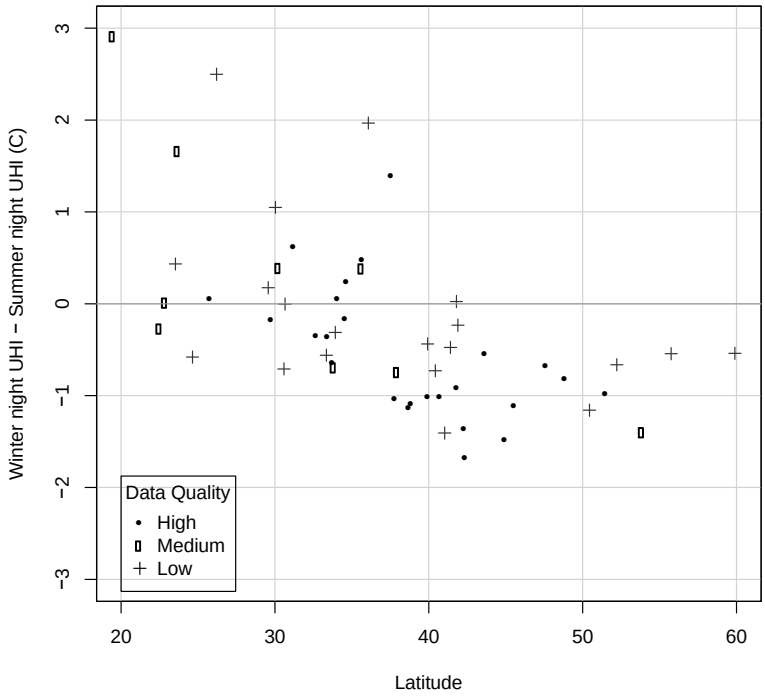

Figure 6. Difference between each city's winter nighttime UHI and summer nighttime UHIs plotted by latitude.

a) b)

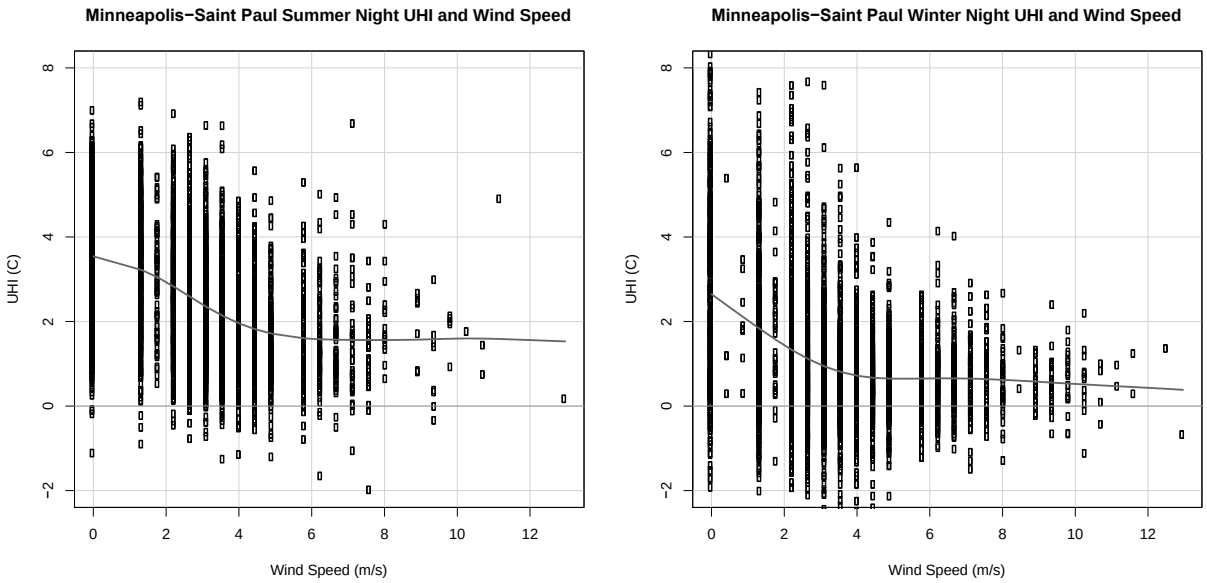

Figure 7. Minneapolis-Saint Paul, MN nighttime UHI and wind speed
Plots of simultaneous wind speed and UHI magnitude for summer (a) and winter (b) nighttime (2300-0400 LST)

Chicago, IL

(a) Overcast sky cover UHI

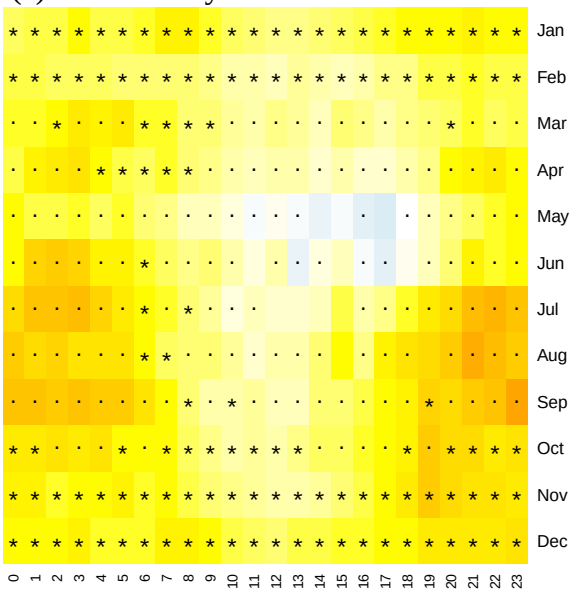

(b) Clear/scattered sky cover UHI

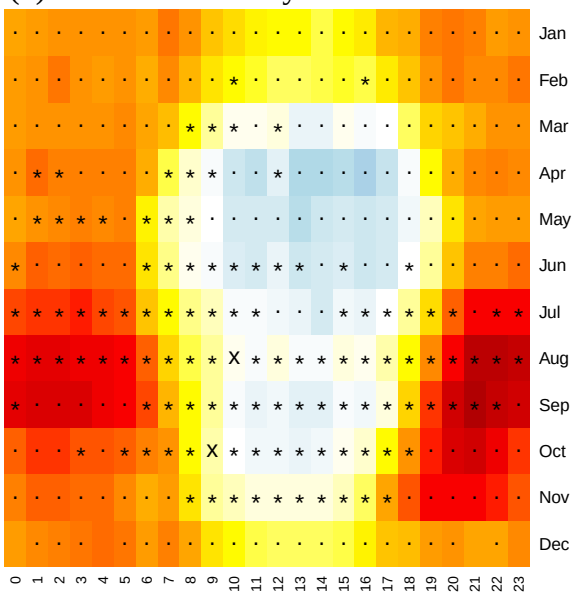

(c) Clear/Scattered – Overcast Difference

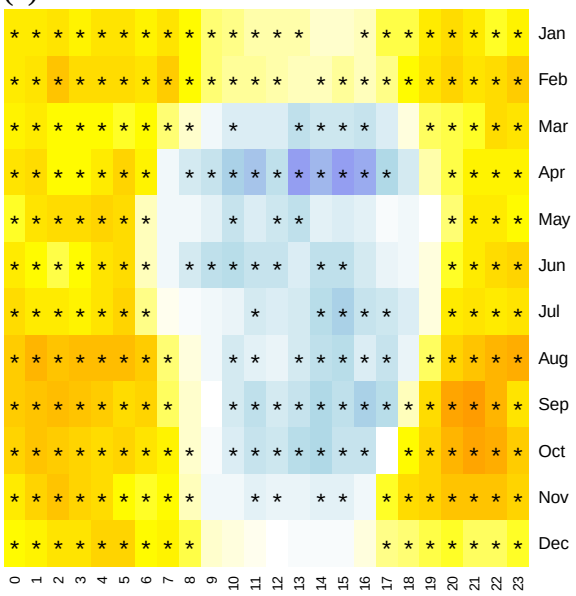

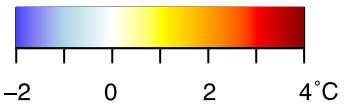

Figure 8. Chicago, IL UHI and sky cover

The magnitude of the Chicago UHI by hour and month under overcast sky cover, clear or scattered sky cover and the clear/scattered – overcast difference. For a and b marks in each month-hour point represent the 95% confidence interval in the UHI magnitude: (.) ± 0.5 ˚C (*) ±0.25 ˚C (X) .125 ˚C. For c the (*) shows that the UHI difference between the two conditions is significant at the 95% confidence interval.

(a) (b)

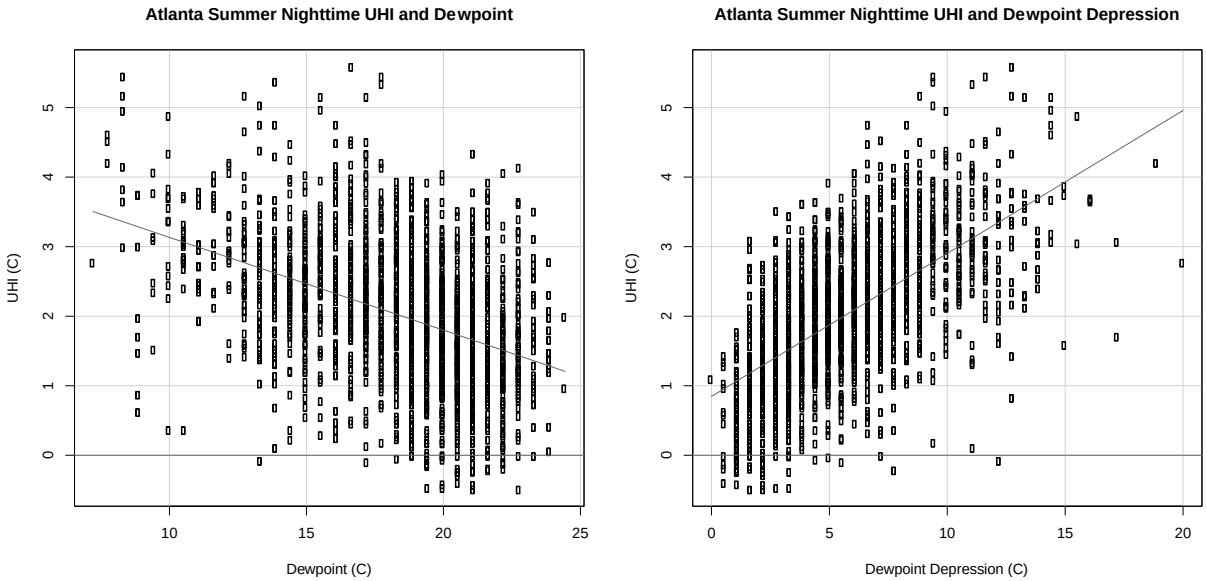

Figure 9. Atlanta, GA UHI and dewpoint temperature
Scatterplot of a) summer nighttime UHI and dewpoint temperature measurements and b) summer nighttime dewpoint depression and UHI for Atlanta under clear or scattered conditions with the linear regression line plotted.

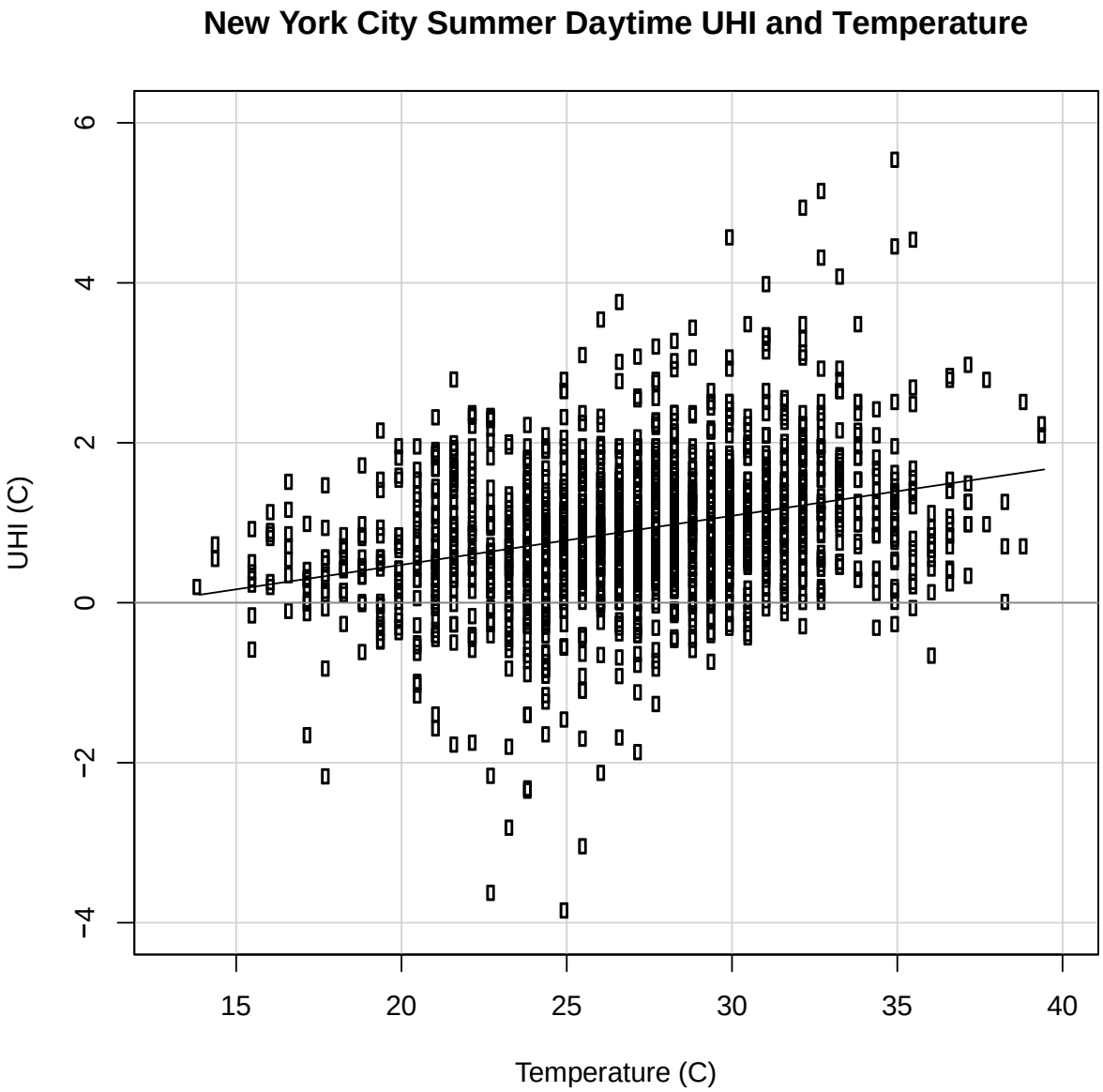

Figure 10. New York City, NY summer daytime UHI and temperature
Scatterplot of all summer afternoon (1400-1600 local time) UHI and temperature measurements for New York City

New York City, NY

(a) Warm Weather UHI

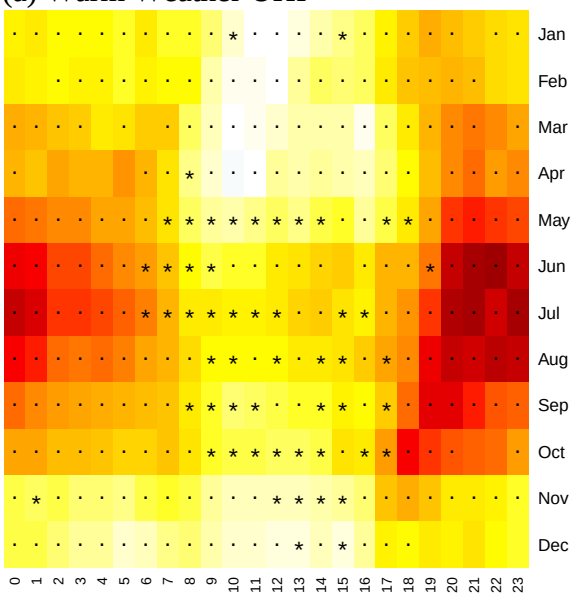

(b) Cold Weather UHI

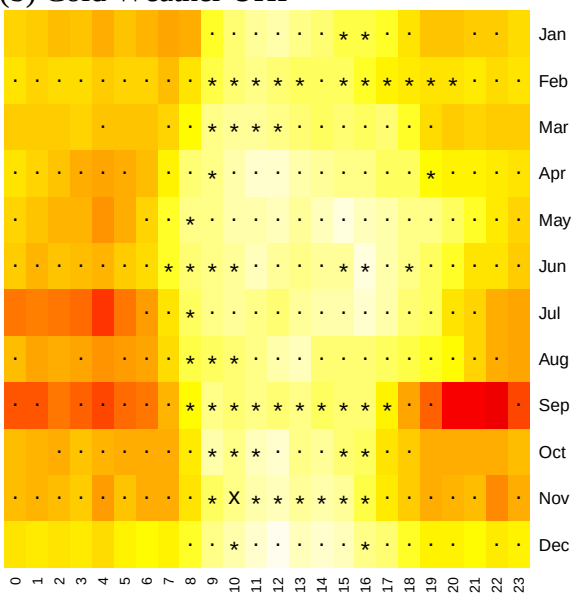

(c) Warm UHI – Cold UHI Difference

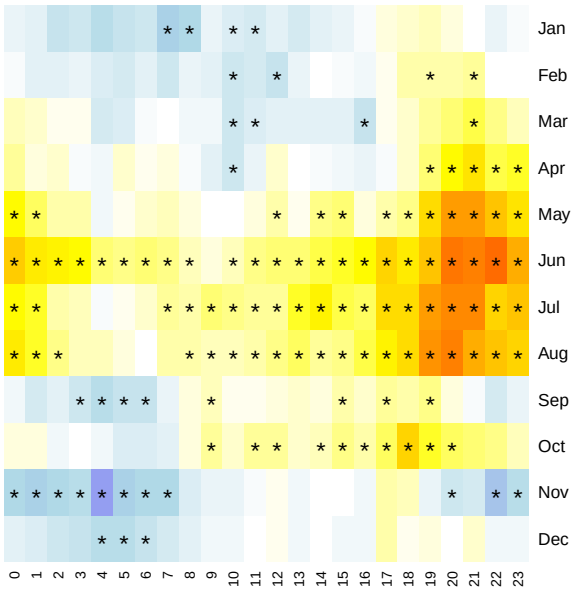

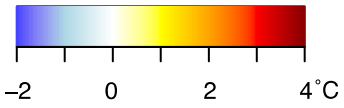

Figure 11. New York City, NY UHI and temperature

The magnitude of the New York City UHI by hour and month in (a) hot events (temperature >1 SD above average), (b) cold events (<1 SD below average) and (c) hot - cold UHI difference.

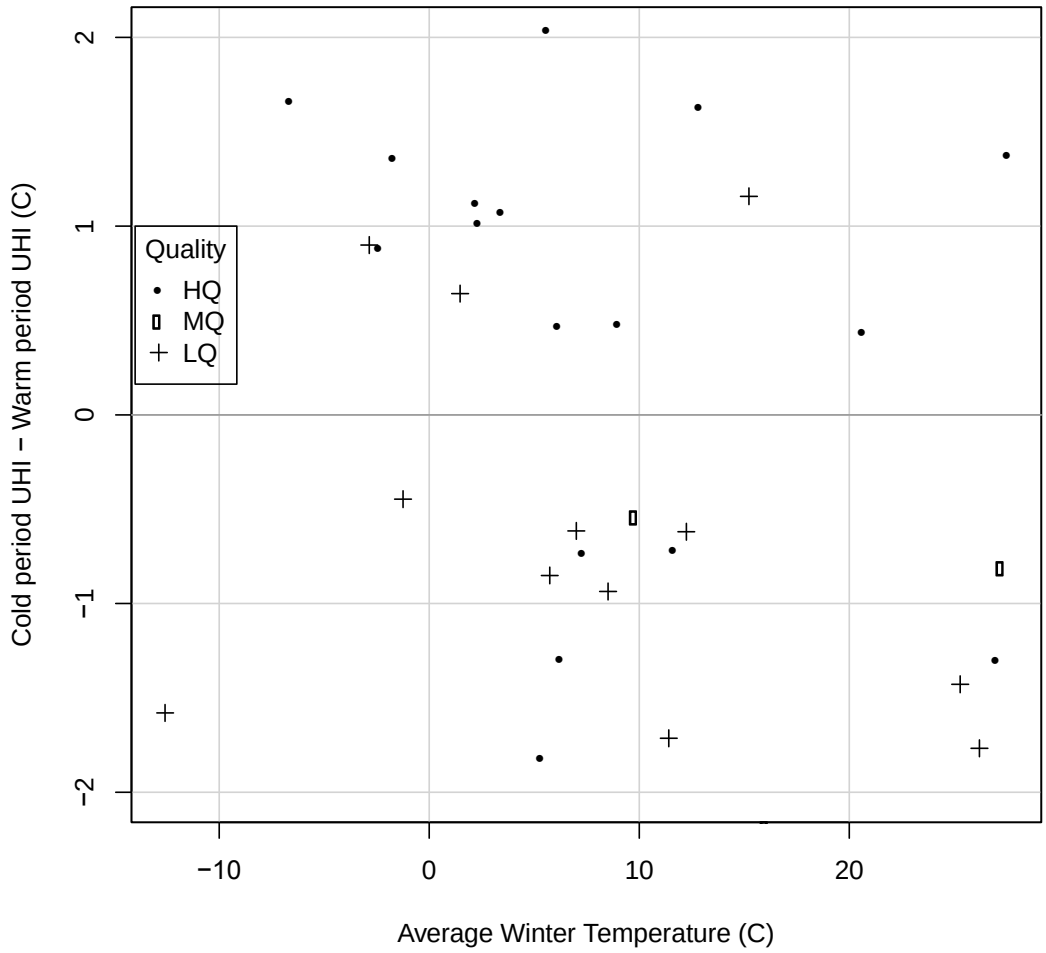

Figure 12. Winter night UHI difference between warm events and cold events by mean winter temperature

Plot of the difference in the UHI between cold events (temperature 1 SD below normal) and hot events (Temperature 1 SD above normal) during winter nights with clear/scattered sky cover and wind < 5m/s as a function of the mean winter temperature over the study period. Only cities with a significant difference in the mean UHI between the two conditions are shown ($p < 0.01$)

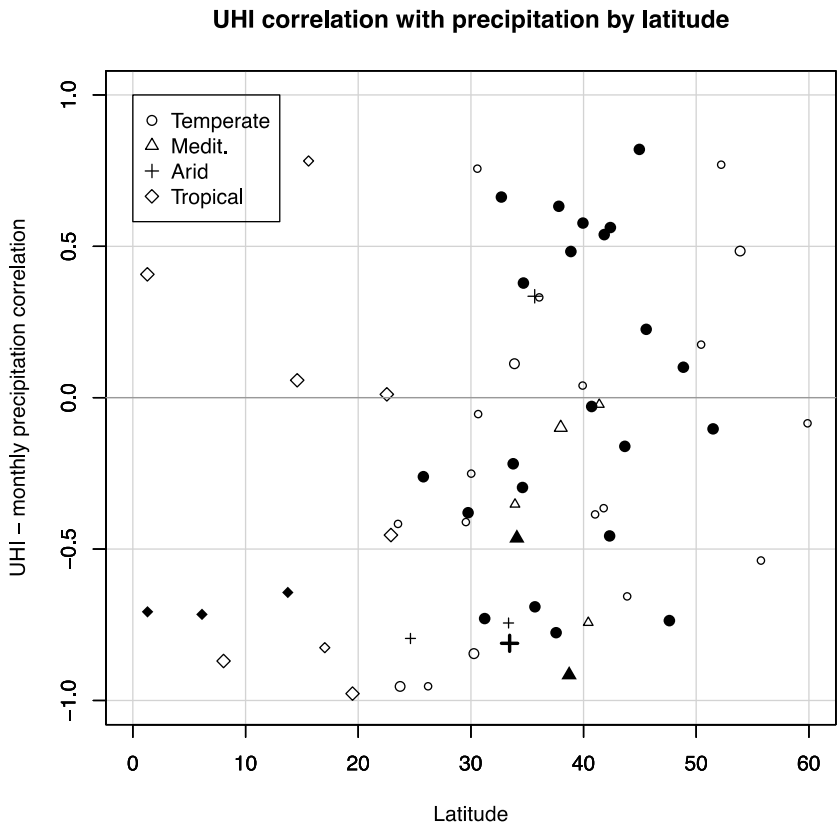

Figure 13. Precipitation and UHI correlation by latitude and biome
Correlation for all months between average monthly precipitation and average monthly nighttime UHI (clear/scattered sky cover, wind <5 m s^{-1}) for each city. Small symbols indicate low quality data, larger symbols indicate medium quality, filled/bold symbols represent high quality data.

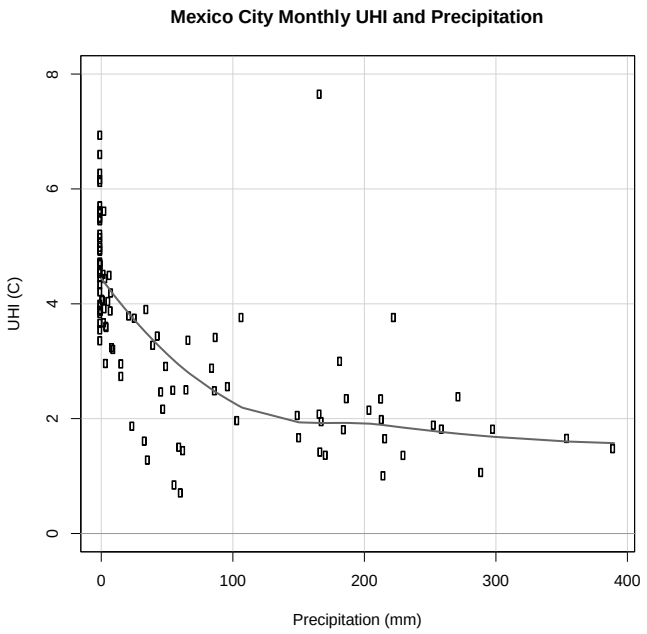

Figure 14. Mexico City, Mexico individual month UHI and precipitation
Nighttime UHI magnitude (clear/scattered sky cover, wind <5 m s^{-1}) and monthly precipitation for Mexico City

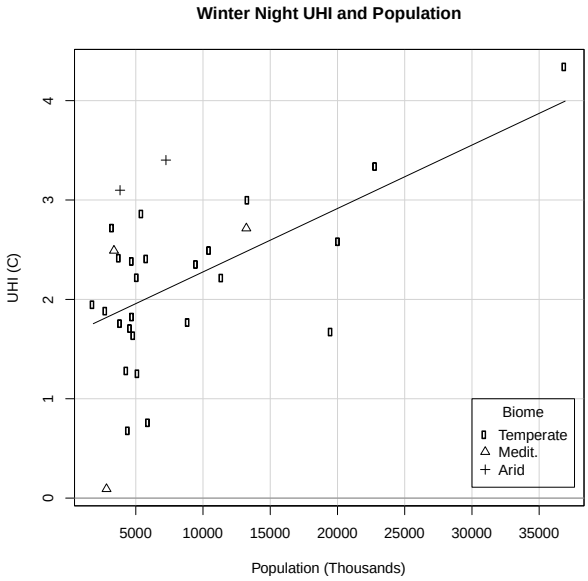

Figure 15. Average winter nighttime UHI of extratropical cities and population, grouped by biome with linear regression trend for all cities.

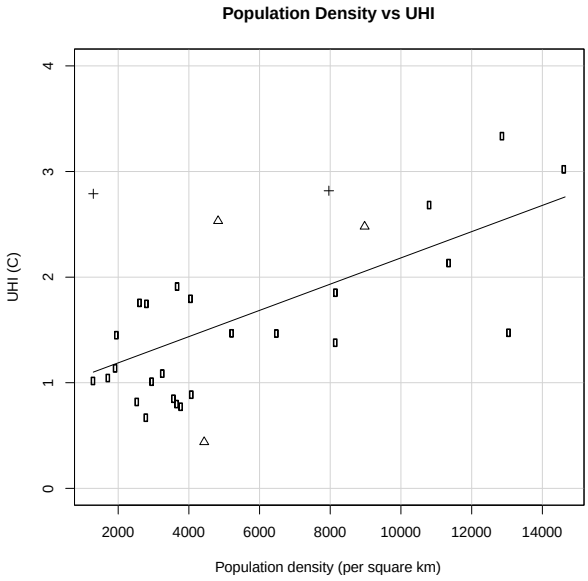

Figure 16. Average winter nighttime UHI of extratropical cities and population density, grouped by biome with linear regression trend for all cities.

(a) (b)

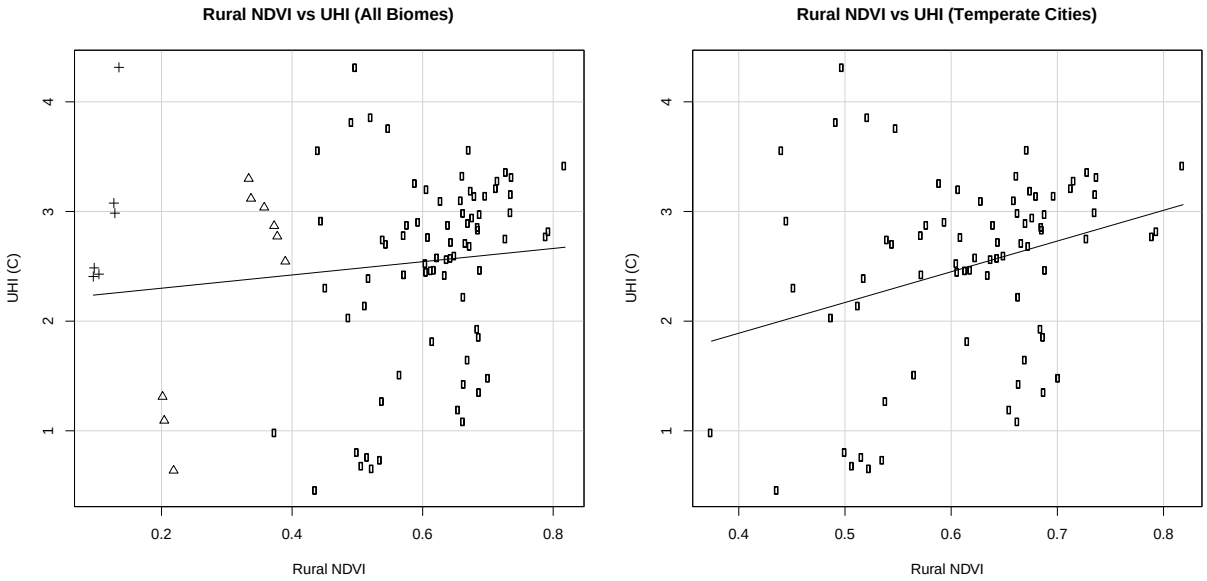

Figure 17. Summer monthly rural NDVI and nocturnal UHI for (a) all biomes and (b) temperate cities with linear regression trend.

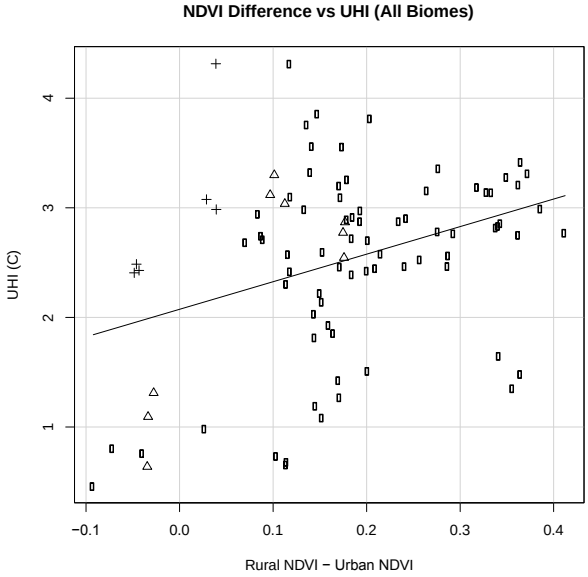

Figure 18. Summer monthly rural – urban NDVI difference and nocturnal UHI for all cities with linear regression trend.

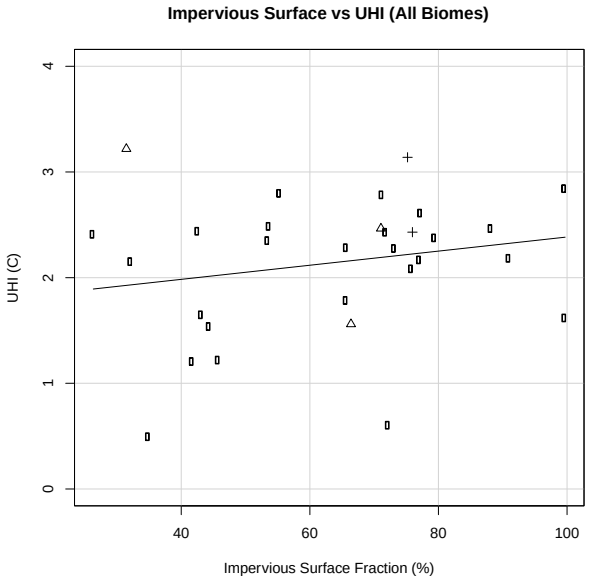

Figure 19. Impervious surface fraction and summer nocturnal UHI for all cities with linear regression trend.

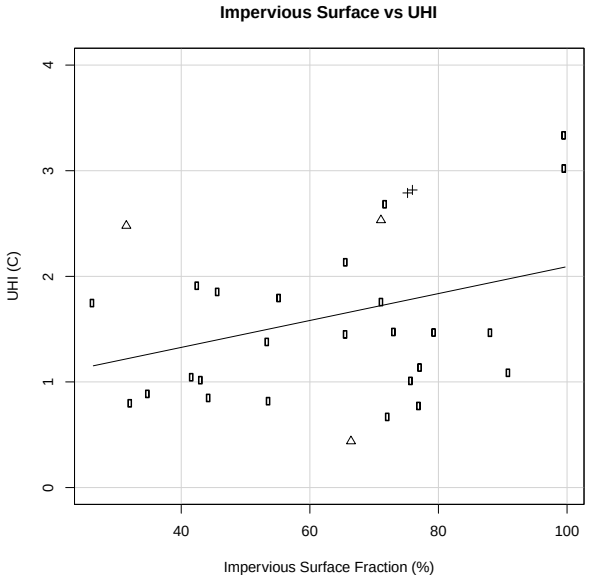

Figure 20. Average winter nighttime UHI of extratropical cities and impervious surface fraction, grouped by biome with linear regression trend for all cities.

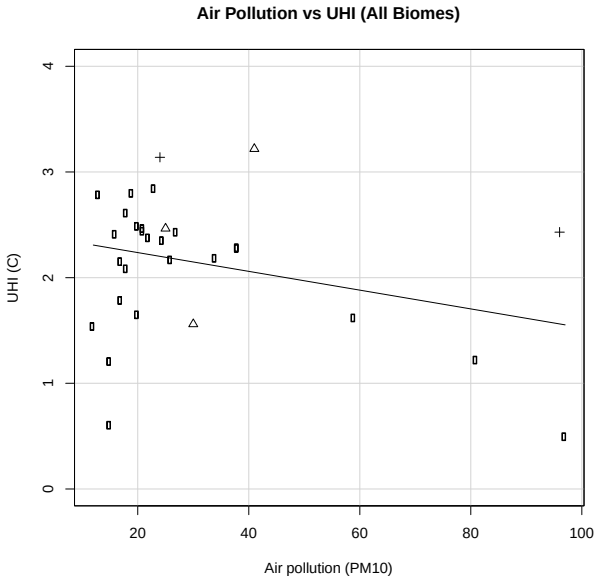

Figure 21. PM10 air pollution and summer nocturnal UHI for all cities with linear regression trend.

Bibliography

Arnfield, A. J., 2003: Two decades of urban climate research: A review of turbulence, exchanges of energy and water, and the urban heat island. *Int J Climatol*, **23,** 1-26.

Arnfield, A. J., and C. S. B. Grimmond, 1998: An urban canyon energy budget model and its application to urban storage heat flux modeling. *Energ Buildings*, **27,** 61-68.

Berry, F. A., E. Bollay, and N. R. Beers, 1945: *Handbook of meteorology.* 1st ed. McGraw-Hill book company, inc., ix, 1068 p. incl. illus. (incl. charts) tables, diagrs. (part fold.) pp.

Brazel, A., N. Selover, R. Vose, and G. Heisler, 2000: The tale of two climates - Baltimore and Phoenix urban LTER sites. *Climate Res*, **15,** 123-135.

Center for International Earth Science Information Network - CIESIN - Columbia University, and Centro Internacional de Agricultura Tropical - CIAT, 2005: Gridded Population of the World, Version 3 (GPWv3): Population Density Grid. NASA Socioeconomic Data and Applications Center (SEDAC).

Christen, A., and R. Vogt, 2004: Energy and radiation balance of a central European city. *Int J Climatol*, **24,** 1395-1421.

Curriero, F. C., K. S. Heiner, J. M. Samet, S. L. Zeger, L. Strug, and J. A. Patz, 2002: Temperature and mortality in 11 cities of the eastern United States. *Am J Epidemiol*, **155,** 80-87.

Elvidge, C. D., and Coauthors, 2007: Global distribution and density of constructed impervious surfaces. *Sensors-Basel*, **7,** 1962-1979.

Estournel, C., R. Vehil, D. Guedalia, J. Fontan, and A. Druilhet, 1983: Observations and Modeling of Downward Radiative Fluxes (Solar and Infrared) in Urban Rural-Areas. *J Clim Appl Meteorol*, **22,** 134-142.

Fan, H. L., and D. J. Sailor, 2005: Modeling the impacts of anthropogenic heating on the urban climate of Philadelphia: a comparison of implementations in two PBL schemes. *Atmos Environ*, **39,** 73-84.

Fouillet, A., and Coauthors, 2006: Excess mortality related to the August 2003 heat wave in France. *Int Arch Occup Environ Health*, **80,** 16-24.

Gaffin, S. R., and Coauthors, 2008: Variations in New York city's urban heat island strength over time and space. *Theor Appl Climatol*, **94,** 1-11.

Gallo, K. P., 2005: Evaluation of temperature differences for paired stations of the US climate reference network. *J Climate*, **18,** 1629-1636.

Grimm, N. B., S. H. Faeth, N. E. Golubiewski, C. L. Redman, J. G. Wu, X. M. Bai, and J. M. Briggs, 2008: Global change and the ecology of cities. *Science*, **319,** 756-760.

Grimmond, C. S. B., and T. R. Oke, 1999: Heat storage in urban areas: Local-scale observations and evaluation of a simple model. *J Appl Meteorol*, **38,** 922-940.

Hirano, Y., and T. Fujita, 2012: Evaluation of the impact of the urban heat island on residential and commercial energy consumption in Tokyo. *Energy*, **37,** 371-383.

Holmer, B., S. Thorsson, and I. Eliasson, 2007: Cooling rates, sky view factors and the development of intra-urban air temperature differences. *Geogr Ann A*, **89A,** 237-248.

Howard, L., 1833: *Climate of London.* 2d. ed.

Huete, A., K. Didan, T. Miura, E. P. Rodriguez, X. Gao, and L. G. Ferreira, 2002: Overview of the radiometric and biophysical performance of the MODIS vegetation indices. *Remote Sens Environ*, **83,** 195-213.

Ichinose, T., K. Shimodozono, and K. Hanaki, 1999: Impact of anthropogenic heat on urban climate in Tokyo. *Atmos Environ*, **33,** 3897-3909.

Imhoff, M. L., P. Zhang, R. E. Wolfe, and L. Bounoua, 2010: Remote sensing of the urban heat island effect across biomes in the continental USA. *Remote Sens Environ*, **114,** 504-513.

Imhoff, M. L., L. Bounoua, R. DeFries, W. T. Lawrence, D. Stutzer, C. J. Tucker, and T. Ricketts, 2004: The consequences of urban land transformation on net primary productivity in the United States. *Remote Sens Environ*, **89,** 434-443.

Jacob, D. J., 1999: *Introduction to atmospheric chemistry.* Princeton University Press, xii, 266 p. pp.

Jauregui, E., 1997: Heat island development in Mexico City. *Atmos Environ*, **31,** 3821-3831.

Jauregui, E., and E. Luyando, 1999: Global radiation attenuation by air pollution and its effects on the thermal climate in Mexico City. *Int J Climatol*, **19,** 683-694.

Jenerette, G. D., S. L. Harlan, W. L. Stefanov, and C. A. Martin, 2011: Ecosystem services and urban heat riskscape moderation: water, green spaces, and social inequality in Phoenix, USA. *Ecol Appl*, **21,** 2637-2651.

Jenerette, G. D., S. L. Harlan, A. Brazel, N. Jones, L. Larsen, and W. L. Stefanov, 2007: Regional relationships between surface temperature, vegetation, and human settlement in a rapidly urbanizing ecosystem. *Landscape Ecol*, **22,** 353-365.

Johnson, D. B., 1985: Urban Modification of Diurnal Temperature Cycles in Birmingham, Uk. *J Climatol*, **5,** 221-225.

Kanda, M., 2007: Progress in urban meteorology: A review. *J Meteorol Soc Jpn*, **85B,** 363-383.

Karl, T. R., H. F. Diaz, and G. Kukla, 1988: Urbanization: Its Detection and Effect in the United States Climate Record. *J Climate*, **1,** 1099-1123.

Laaidi, K., A. Zeghnoun, B. Dousset, P. Bretin, S. Vandentorren, E. Giraudet, and P. Beaudeau, 2012: The impact of heat islands on mortality in Paris during the August 2003 heat wave. *Environ Health Persp*, **120,** 254-259.

Landsberg, H. E., 1981: *The urban climate.* Academic Press, x, 275 p. pp.

Lin, G. C. S., 1994: Changing Theoretical Perspectives on Urbanization in Asian Developing-Countries. *Third World Plan Rev*, **16,** 1-23.

Manley, G., 1958: On the frequency of snowfall in metropolitan England. *Q J Roy Meteor Soc*, **84,** 70-72.

Mishra, V., and D. P. Lettenmaier, 2011: Climatic trends in major US urban areas, 1950-2009. *Geophys Res Lett*, **38**.

Montgomery, M. R., 2008: The urban transformation of the developing world. *Science*, **319,** 761-764.

Moriwaki, R., and M. Kanda, 2004: Seasonal and diurnal fluxes of radiation, heat, water vapor, and carbon dioxide over a suburban area. *J Appl Meteorol*, **43,** 1700-1710.

Morris, C. J. G., and I. Simmonds, 2000: Associations between varying magnitudes of the urban heat island and the synoptic climatology in Melbourne, Australia. *Int J Climatol*, **20,** 1931-1954.

Morris, C. J. G., I. Simmonds, and N. Plummer, 2001: Quantification of the influences of wind and cloud on the nocturnal urban heat island of a large city. *J Appl Meteorol*, **40,** 169-182.

National Climatic Data Center/NESDIS/NOAA/ U.S. Department of Commerce, Air Force Combat Climatology Center/U.S. Air Force/U.S. Department of Defense, and Air Force Weather Agency/U.S. Air Force/U.S. Department of Defense..,

2005: NCDC TD3505 Integrated Surface Hourly Data, 1901-continuing. Research Data Archive at the National Center for Atmospheric Research, Computational and Information Systems Laboratory, Boulder, Colo., Ed., National Climatic Data Center. Accessed 1 Dec 2013

Oke, T. R., 1981: Canyon Geometry and the Nocturnal Urban Heat-Island - Comparison of Scale Model and Field Observations. *J Climatol*, **1,** 237-&.

——, 1982: The Energetic Basis of the Urban Heat-Island. *Q J Roy Meteor Soc*, **108,** 1-24.

——, 1987: *Boundary layer climates.* 2nd ed. Methuen, xxiv, 435 p. pp.

——, 1988: The Urban Energy-Balance. *Prog Phys Geog*, **12,** 471-508.

Olson, D. M., and Coauthors, 2001: Terrestrial ecoregions of the worlds: A new map of life on Earth. *Bioscience*, **51,** 933-938.

Park, H. S., 1986: Features of the Heat-Island in Seoul and Its Surrounding Cities. *Atmos Environ*, **20,** 1859-1866.

Pearlmutter, D., P. Berliner, and E. Shaviv, 2005: Evaluation of urban surface energy fluxes using an open-air scale model. *J Appl Meteorol*, **44,** 532-545.

Peters, E. B., R. V. Hiller, and J. P. McFadden, 2011: Seasonal contributions of vegetation types to suburban evapotranspiration. *J Geophys Res-Biogeo*, **116**.

Peterson, T. C., 2003: Assessment of urban versus rural in situ surface temperatures in the contiguous United States: No difference found. *J Climate*, **16,** 2941-2959.

Sailor, D. J., 2011: A review of methods for estimating anthropogenic heat and moisture emissions in the urban environment. *Int J Climatol*, **31,** 189-199.

Sailor, D. J., and H. L. Fan, 2002: Modeling the diurnal variability of effective albedo for cities. *Atmos Environ*, **36,** 713-725.

Sailor, D. J., and L. Lu, 2004: A top-down methodology for developing diurnal and seasonal anthropogenic heating profiles for urban areas. *Atmos Environ*, **38,** 2737-2748.

Sailor, D. J., and M. Hart, 2006: An Anthropogenic Heating Database for Major U.S. Cities. *86th AMS Annual Meeting*.

Salamanca, F., M. Georgescu, A. Mahalov, M. Moustaoui, and M. Wang, 2014: Anthropogenic heating of the urban environment due to air conditioning. *Journal of Geophysical Research: Atmospheres*, **119,** 5949-5965.

Schneider, A., M. A. Friedl, and D. Potere, 2009: A new map of global urban extent from MODIS satellite data. *Environ Res Lett*, **4**.

——, 2010: Mapping global urban areas using MODIS 500-m data: New methods and datasets based on 'urban ecoregions'. *Remote Sens Environ*, **114,** 1733-1746.

Souch, C., and S. Grimmond, 2006: Applied climatology: urban climate. *Prog Phys Geog*, **30,** 270-279.

Stanhill, G., and J. D. Kalma, 1995: Solar Dimming and Urban Heating at Hong-Kong. *Int J Climatol*, **15,** 933-941.

Stewart, I. D., 2011: A systematic review and scientific critique of methodology in modern urban heat island literature. *Int J Climatol*, **31,** 200-217.

Stewart, I. D., and T. R. Oke, 2012: Local Climate Zones for Urban Temperature Studies. *B Am Meteorol Soc*, **93,** 1879-1900.

Stone, B., 2005: Urban heat and air pollution - An emerging role for planners in the climate change debate. *J Am Plann Assoc*, **71,** 13-25.

——, 2007: Urban and rural temperature trends in proximity to large US cities: 1951-2000. *Int J Climatol*, **27,** 1801-1807.

Szymanowski, M., 2005: Interactions between thermal advection in frontal zones and the urban heat island of Wroclaw, Poland. *Theor Appl Climatol*, **82,** 207-224.

Taha, H., S. Konopacki, and S. Gabersek, 1999: Impacts of large-scale surface modifications on meteorological conditions and energy use: A 10-region modeling study. *Theor Appl Climatol*, **62,** 175-185.

Tremeac, B., and Coauthors, 2012: Influence of air conditioning management on heat island in Paris air street temperatures. *Appl Energ*, **95,** 102-110.

UN, 2011: World Urbanization Prospects: The 2011 Revision, Highlights. United Nations Department of Economic and Social Affairs/Population Division

Unger, J., 2004: Intra-urban relationship between surface geometry and urban heat island: review and new approach. *Climate Res*, **27,** 253-264.

Whitman, S., G. Good, E. R. Donoghue, N. Benbow, W. Shou, and S. Mou, 1997: Mortality in Chicago attributed to the July 1995 heat wave. *Am J Public Health*, **87,** 1515-1518.

WHO, 2011: Urban outdoor air pollution database. September 2011 ed., Department of Public Health, World Health Organization.

Yamashita, S., 1990: The Urban Climate of Tokyo. *Geographical Review of Japan*, **63,** 98-107.

Appendix

City	Rural Station IDs	Urban Station IDs
Ankara, Turkey	171280	171295, 171290
Athens, Greece	166990, 166650	167180, 167160
Atlanta, USA	722197, 747809, 722156	722195, 722270, 722196, 722190
Baghdad, Iraq	691144	691734
Bangalore, India	427056	432950
Bangkok, Thailand	484300, 484270, 484580, 484640	484550, 484530, 484540, 484560
Barcelona, Spain	81840	81810
Beunos Aires, Argentina	875760, 875930	875820, 875710
Boston, USA	725068, 722256, 725064	725090
Cape Town, RSA	687140	688160
Changchun, China	509490, 540490	541610
Chengdu, China	561870	562940
Chicago, USA	744655, 7201377, 725347, 722075	725300, 997255, 725340
Chonqing, China	576040, 574110	575160
Dallas, USA	722589, 722489	722590, 722580, 722583
Detroit, USA	725374, 725404, 725378, 721980, 725384	725370, 725375
Dhaka, Bangladesh	427240	419230, 419220
Hangzhou, China	585560, 583450	584570
Houston, USA	722444, 722351, 722527	722436, 722430, 722543
Istanbul, Turkey	172005, 170575	170600
Jakarta, Indonesia	967390, 967490, 967370	967410, 967450
Johannesburg, RSA	683500, 680007, 683490, 682550	683680, 682672, 687671
Khartoum, Sudan	627500, 627510	627210
Kiev, Ukraine	333470	333450
Kunming, China	567860, 568860, 567680, 566840	567780
Lisbon, Portugal	85340, 85410	85350, 85360, 85790
London, UK	37810, 36840, 37690	37683

Los Angeles, USA	723910, 722926, 723927	994035, 722956, 722970, 722950, 722874, 722955, 722885
Madrid, Spain	82270	82210
Manila, Philippines	984260, 984320	984290, 984250
Melbourne, Australia	948955, 948630, 948980, 948540	948680
Mexico City, Mexico	766750, 766830	766800, 766810
Miami, USA	722026, 722189	722039, 722020, 722037, 722024
Minneapolis – Saint Paul, USA	726682, 722418, 727503, 722003, 727517, 722179, 722144, 726418	726580, 726584
Minsk, Belorus	261148	268500
Montreal, Canada	717120, 716140, 711840	716270, 716120
Moscow, Russia	370008	276120
Nairobi, Kenya	637200, 637140, 637170	637420
New York City, USA	725016, 997289, 724077, 725037, 724084	725025, 997271, 744860, 725030, 725020
Osaka-Kobe, Japan	476490, 477800	477710, 477720, 477700
Paris, France	70570, 71530	71560
Philadelphia, USA	720324, 725113, 724090, 724096	997286, 724085, 724080
Phoenix, USA	722748	722780
Porto Alegre, Brazil	839850	839710
Qingdao, China	548630	548570
Recife, Brazil	827980, 829930	828990
Rio De Janeiro, Brazil	837410	837480, 837460, 837550
Riyadh, Saudi Arabia	404370	404380
Saint Petersburg, Russia	260590, 228920	260630
Sao Paolo, Brazil	837210, 838093	837800
Seattle, USA	994025, 727945, 727928	994350, 727930, 994014, 727935
Seoul, South Korea	470980, 471010, 470990, 471220	471080
Shanghai, China	582650, 582510, 583450	583620, 583670
Shenyang, China	542360, 541570	543420
Shenzhen, China	595010, 450320, 596630, 592930	594930

Singapore, Singapore	486021, 486790	486990, 486980, 486940
Sydney, Australia	947590, 947480	947680, 947670
Tehran, Iran	407807, 407300	407540
Tokyo, Japan	476860, 477160	476620, 476713
Toronto, Canada	712960, 713680, 715340, 714310	712650, 715080, 712643
Warsaw, Poland	124900, 122700, 124880, 124690, 123850, 123760	123750
Washington, USA	724057, 724043, 724035, 720317	724050, 997314
Wuhan, China	573990, 574760	574940
Yangon, Myanmar	480940	480970

A1. List of meteorological station IDs used from the Integrated Surface Hourly data set.